Controls on propagation of the Indian monsoon onset in an idealised model

Received: 10 April 2021 | Revised: 24 August 2021 | Accepted: 25 August 2021

DOI: 10.1002/qj.4165

Quarterly Journal of the Royal Meteorological Society RMetS

RESEARCH ARTICLE

Controls on propagation of the Indian monsoon onset in an idealised model

Lucy G. Recchia[1] | **Stephen D. Griffiths**[2] | **Douglas J. Parker**[3]

[1]Department of Mathematics and Statistics, University of Reading, Reading, UK

[2]School of Mathematics, University of Leeds, Leeds, UK

[3]School of Earth and Environment, University of Leeds, Leeds, UK

Correspondence
L. G. Recchia, Department of Mathematics and Statistics, University of Reading, Reading, RG6 6AX, UK.
Email: l.g.recchia@reading.ac.uk

Funding information
Horizon 2020 EU project TiPES UK NERC Leeds-York DTP INCOMPASS project Royal Society Wolfson Research Merit Award (2014–2018), Grant/Award Numbers: 820970, NE/L002574/1, NE/L013843/1

Abstract

The Indian monsoon is a seasonal large-scale circulation system with complex dynamical and thermodynamic interactions. The physical processes are not fully understood. In particular, the mechanisms that control the propagation of the monsoon onset across the Indian continent, against the mid-level wind field, are debated. The Indian monsoon is poorly represented in weather and climate models, with persistent systematic errors making it difficult to forecast the Indian monsoon accurately on subseasonal timescales. A two-layer model based on moisture conservation with a parameterised flux representing convection is developed and used to investigate the competition between dry advection in the upper levels, the rate of moisture replenishment at low levels, and the rate of convection from the lower to the upper layers. In a fixed Eulerian frame, the system is initialised at an equilibrium representing pre-onset (May) conditions. Then, changes in the rates of moist inflow and upper-level advection are introduced, triggering a transition to a new equilibrium, which reflects the full monsoon state (July–September). The two-layer model reproduces the Indian monsoon onset and its progression to the northwest, against an imposed $5\,\mathrm{m\cdot s^{-1}}$ wind in the upper layer. Increasing the parameter representing moist inflow induces a monsoon onset, defined as a threshold of total column moisture, with clear progression from southeast toward northwest India. A lesser wind speed in the upper layer, signifying a weakening midtropospheric dry intrusion, allows more rapid progression of the monsoon onset. A greater upper-level wind speed, associated with a strengthening dry intrusion, causes the monsoon onset to retreat. We can quantify the nature of the monsoon onset by deriving an onset speed and the time taken for the system to adjust to a new equilibrium, using analytical theory.

KEYWORDS

climate change, convection, idealised model, Indian monsoon, moisture budget, monsoon onset, weather

1 | INTRODUCTION

The Indian monsoon is a globally significant meteorological event, bringing around 80% of India's annual rainfall between the months of June and September. Accurate prediction of the monsoon onset and associated rainfall on a regional scale is important for agriculture, industry, and the Indian economy (Kumar *et al.*, 2004; Gadgil and Gadgil, 2006; Gadgil and Rupa Kumar, 2006). The monsoon is initiated in May by a change in large-scale circulation, which allows an influx of moisture from the Arabian Sea, helping to create an environment favourable for convection and enhanced precipitation (McGregor and Nieuwolt, 1998; Zhang *et al.*, 2004; Ding and Sikka, 2006; Hoskins and Wang, 2006). The monsoon onset, heralding the start of the rainy season, is typically declared on June 1 in the southwest state of Kerala, with a standard deviation of 8 days (Joseph *et al.*, 2006). Specific criteria regarding the rainfall, wind speed/pressure, and outgoing longwave radiation need to be met before onset is declared in a particular region (India Meteorological Department, 2016). Once the monsoon has first onset in Kerala, the onset progresses from southeast to northwest India over the following 5–6 weeks. The onset progression can be seen from Figure 1, where the dotted lines represent isochrones of monsoon onset from climatology. Initially, the onset progresses rapidly from Kerala to covering all of southern India in about 2 weeks. Then the advance slows, taking a further 4 weeks for onset to be declared in the northwestern state of Rajasthan. The onset progresses faster on the west coast and at the northeastern border with the Himalayas than over central India. Using the length of India (≈ 3,000 km) and the time taken for the onset to progress (≈ 6 weeks), an approximate onset speed of 1 m·s^{-1} can be calculated.

The Indian monsoon system is particularly interesting in that the direction of onset propagation opposes the mid-level wind field. At the time of monsoon onset, low-level winds are southwesterly, conveying moisture from the Arabian Sea. Mid-level winds are northwesterly and typically dry, with moisture availability being low over arid northwest India. At higher levels, the Tropical Easterly Jet forms over north India initially, then spreads across India as the monsoon develops. Referring to the wind profile over northwest India shown in Figure 2, strong northwesterly winds at 400–200 hPa dominate at the time of onset (May 31). As the monsoon onset progresses to the northwest, a corresponding decrease in the northwesterly wind speed at mid to high levels is observed. For example, at 400 hPa, the wind speed reduces from approximately 10 m·s^{-1} just before first onset (May 31) to 5 m·s^{-1} at mid-onset (June 15) to 0 m·s^{-1} during the full monsoon (July 15). In the layer 900–500 hPa, the northwesterly

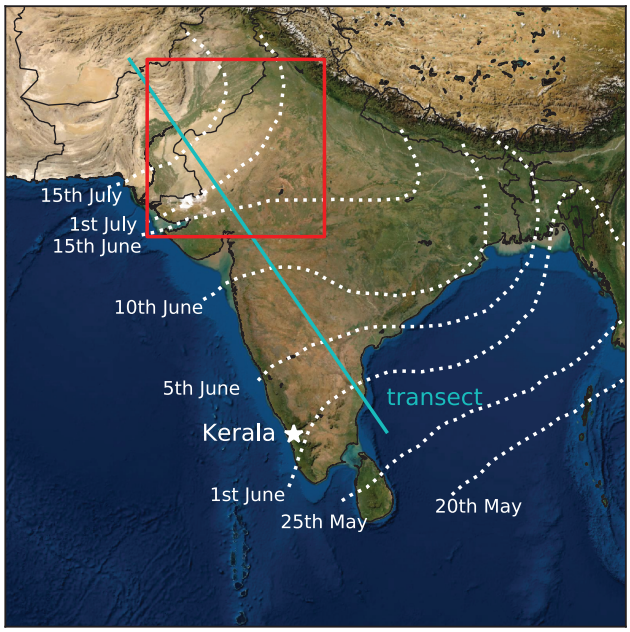

FIGURE 1 Schematic showing the progression of the Indian monsoon onset from southeast to northwest India. The isochrones (dotted lines) of onset dates highlight the nonlinear nature of the advance. The location of Kerala, an important landmark for monsoon onset, is indicated by the white star. The redbox shows the area used to compute the northwesterly wind profile in Figure 2. A transect from north to south India is shown by the cyan line. Satellite image from ArcGIS

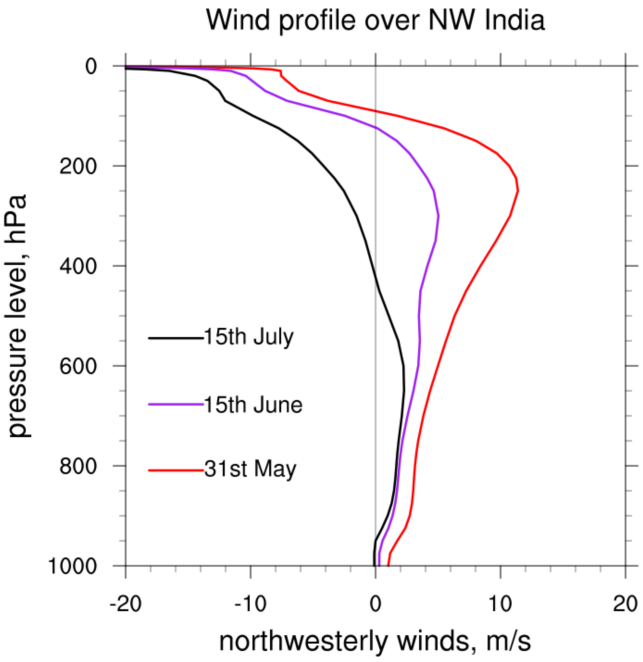

FIGURE 2 Vertical wind profile for northwest India, averaged over the box 22°N, 68°E–32°N, 78°E (shown in Figure 1), produced from ERA-Interim reanalysis (1988–2017). Northwesterly component of winds averaged over 5-day periods centred on May 31 (first onset, red), June 15 (mid-onset, purple), and July 15 (full monsoon, black)

component persists. Near the surface, the northwesterly wind speed remains small ($< 1\,\mathrm{m\cdot s^{-1}}$) throughout the monsoon period.

A theory of the propagation of monsoon onset is described in Parker *et al.* (2016) based on observations, but without quantitative testing. Parker *et al.* (2016) focus on the competition between a dry intrusion at mid-levels and the moistening processes leading to monsoon onset. Moist inflow at low levels supports shallow convection over India, eroding the wedge of dry air and encouraging the advance of the onset to the northwest. There is a significant increase in moisture over southeast India, with a shallow moist layer approximately doubling in extent and depth between pre-onset and the full monsoon.

A strengthening of the dry intrusion can inhibit the northwestern propagation of the monsoon onset, instigating dry spells known as monsoon breaks (Krishnamurti *et al.*, 2010). The role of the mid–upper troposphere (200–500 hPa) in the strength and variation of the Indian monsoon is also highlighted by Dai *et al.* (2013), specifically referring to the land–ocean thermal contrast at mid–upper levels. From observational analysis, Saini *et al.* (2011) identified large-scale temperature advection and vertical motion as key factors in determining the inland development of the monsoon and the strength of the onset. Bollasina and Ming (2013b) emphasised the importance of the interaction between soil moisture and circulation, demonstrating that a northwestward progression of the monsoon can be simulated through the evolution of land-surface processes, with other factors such as sea-surface temperatures and insolation fixed in a May-like state. The increase in aerosols over recent years, primarily from biomass burning, has been linked with earlier monsoon onsets (Bollasina *et al.*, 2013). There is some debate on whether black carbon aerosols act to enhance or delay the monsoon onset (e.g., Meehl *et al.*, 2008; Mahmood and Li, 2013). Although land-surface processes and aerosol interactions affect the dynamics of monsoon onset, here we focus exclusively on the role of atmospheric moisture processes.

The complex dynamical nature of the Indian monsoon is not well understood and the physical processes are poorly represented in models, which typically show dry biases in the northwest and have rain falling too extensively and lightly (Stephens *et al.*, 2010; Lucas-Picher *et al.*, 2011; Bollasina and Ming, 2013a; Sperber *et al.*, 2013; Karmacharya *et al.*, 2015; George *et al.*, 2016; Johnson *et al.*, 2017; Martin *et al.*, 2017; Goswami and Goswami, 2017). The skill of prediction of the onset of the monsoon and precipitation on subseasonal timescales is particularly poor compared with other global monsoon systems (Bombardi *et al.*, 2017). Performance of climate models is improving, with the spatial pattern and timing of monsoonal precipitation being captured better in the Coupled Model Intercomparison Project Phase 6 (CMIP-6) multimodel average compared with the CMIP-5 multimodel average, although large variability and discrepancy between individual climate models remains (Gusain *et al.*, 2020). The spatial resolution, choice of boundary conditions, and physical representation of convection—explicit or parameterised—are possible limitations of modelling the onset and progression of the monsoon (Dirmeyer *et al.*, 2012; Holloway *et al.*, 2012; Mishra *et al.*, 2014; Birch *et al.*, 2015; Johnson *et al.*, 2017; Willetts *et al.*, 2017; Gusain *et al.*, 2020). Clearly, there is a need to define the various processes that can influence monsoon onset and to quantify the effects on the speed of onset progression and precipitation pattern/rate, through modelling studies and comparison with observations.

A simple unifying framework is needed to understand the interacting processes leading to monsoon onset, in which the strength of individual contributions and their interactions can be tested and quantified explicitly. Here we develop a simple dynamically consistent model that reproduces the propagation of the monsoon onset. The competition between low-layer moisture supply, parameterised moisture transport between layers, and upper-level advection of moisture is considered. Other effects such as precipitation and vegetation are neglected at present, although we aim to include these additional effects in future work. We use this framework to test the hypothesis presented in the conceptual article by Parker *et al.* (2016), namely whether moisture arguments alone can explain the propagation of the Indian monsoon onset to the northwest, against the mid-level wind field. The model consists of two layers, representing the lower and upper troposphere, in a vertical section running from northwest to southeast India. The key features are an inflow of moisture to the lower layer, representing the monsoon flow, net vertical transport of moisture parameterised simply in terms of upper- and lower-layer moisture, and an upper-level wind, representing a northwesterly dry intrusion. The representation of the vertical moisture flux and the parameters controlling the rates of inflow and advection are to be investigated in relation to different phases of monsoon onset, using metrics such as onset direction and speed of onset propagation.

2 | IDEALISED MODEL OF INDIAN MONSOON ONSET

Figure 3 illustrates the model configuration, which is based on a vertical section running from northwest to southeast India (along the red line in Figure 1), taking x and z axes in the horizontal and vertical directions

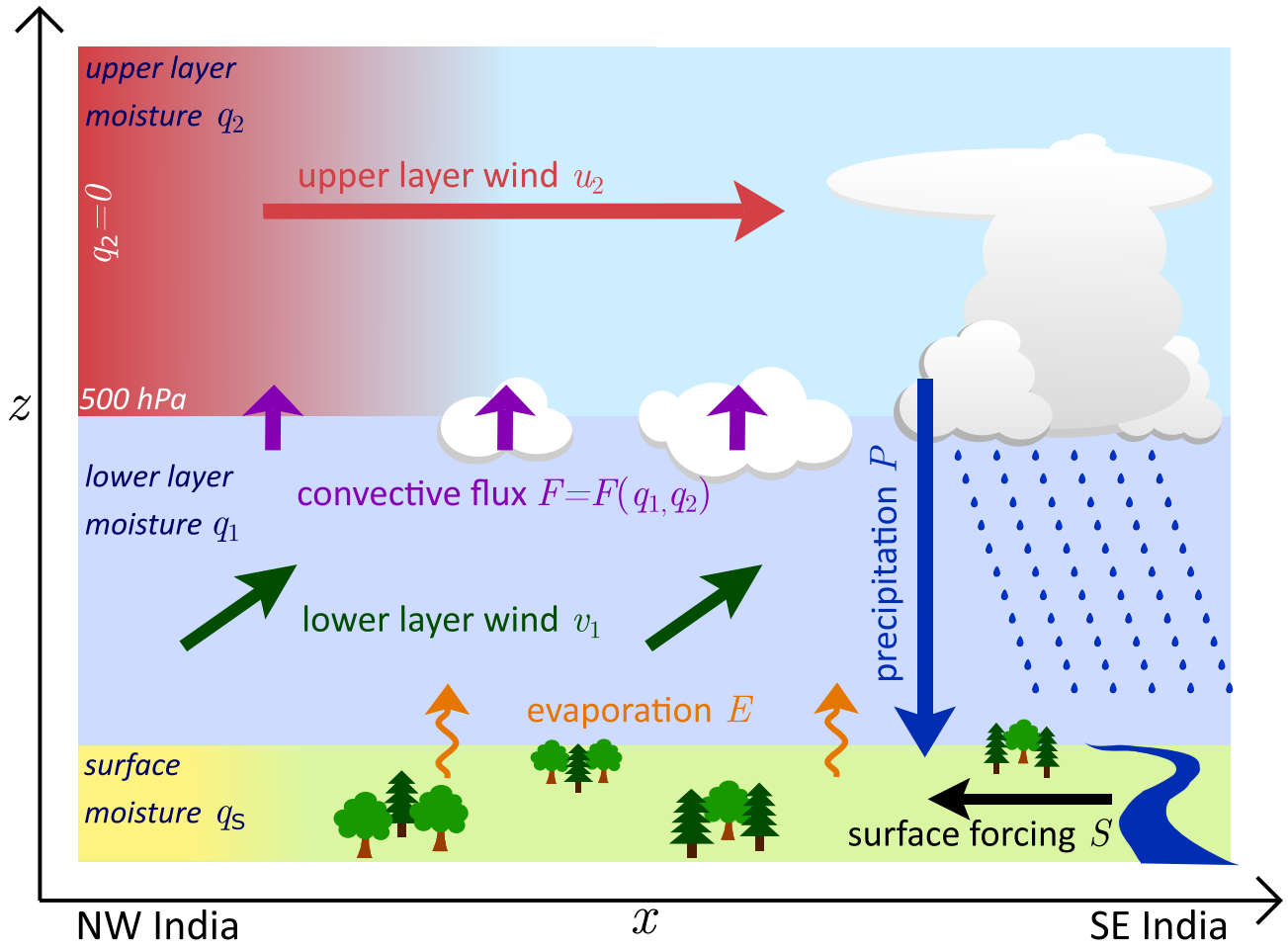

FIGURE 3 Schematic of the multilayer idealised model of Indian monsoon onset. The x direction is in a transect running from northwest to southeast India, with the z direction being vertical into the atmosphere

respectively. The atmosphere is split into two layers of equal depth (i.e., equal mass) at the 500-hPa pressure level, representing the upper and lower troposphere, with a ground level to capture surface processes. The upper layer extends to the top of the atmosphere, which we define as 50 hPa, in line with some atmospheric weather models. Taking a moisture-budget approach, we model the evolution of moisture in each layer by Equations 1a–1c, with q_s, q_1, q_2 being column-integrated moisture content in the surface, lower and upper layers respectively. A threshold of total moisture content $(q_1 + q_2)$ is used to define monsoon onset. As the layers are the same depth, column-integrated quantities are equivalent to layer-mean mixing ratios, which can be recovered by dividing by the layer height. At the surface, water can enter or leave the system through a surface forcing term S, which accounts for the effects of river run-off and convergence from groundwater flow. Moisture lost through evaporation E at the surface is added to the lower-layer moisture budget, and moisture can be exchanged between the lower and upper layers through a convective flux function. Precipitation P occurs in the upper layer only, given that a threshold of column-integrated moisture content q_2 has been reached. Moisture leaving the upper layer as precipitation is transferred instantaneously to the surface, so that there is no residence time in the lower layer.

The horizontal wind field, assumed to be nondivergent, is denoted by $\mathbf{u_1}$ and $\mathbf{u_2}$, where subscripts 1 and 2 refer to the lower and upper atmospheric layers. The predominant winds in the lower layer are southwesterly, bringing moisture from the Arabian Sea, so $\mathbf{u_1} = (0, v_1)$, where the y direction is going into the page (Figure 3). Dry air is advected from northwest India in the upper layer, with $\mathbf{u_2} = (u_2, 0)$, competing against the propagation of the monsoon onset.

$$\frac{\partial q_2}{\partial t} + \mathbf{u_2} \cdot \nabla q_2 = +F - P, \tag{1a}$$

$$\frac{\partial q_1}{\partial t} + \mathbf{u_1} \cdot \nabla q_1 = -F + E, \tag{1b}$$

$$\frac{\partial q_s}{\partial t} = +P - E + S. \tag{1c}$$

The flux of water vapour, F, from the lower layer to the upper layer due to convection must be parameterised. Here we describe the flux in terms of q_1 and q_2 alone. In addition, we need to account for fluxes due to updrafts (linked with cloud formation) and the compensating subsidence and downdrafts. When $q_1 = q_2$, these two processes cannot lead to any net moisture flux, and so $F = 0$. Otherwise, there will be a downgradient flux, that is, $F > 0$ when $q_1 > q_2$ and $F < 0$ when $q_2 > q_1$, although the strength of this flux will depend upon q_1 and q_2 in a nontrivial way. We thus use the simple parameterisation:

$$F = \frac{1}{T_{\text{conv}}}(q_1 - q_2)\,\Phi(q_1, q_2), \text{ where } \Phi = 1. \tag{2}$$

The parameter T_{conv} is the timescale for convective adjustment, and $\Phi(q_1, q_2)$ is a positive nondimensional function representing cloud activity. Together, Φ and T_{conv} represent the rate of growth of shallow cumulus clouds, which are required to supply moisture in order to facilitate the growth of deep, precipitating cumulus clouds (Yanai *et al.*, 1973). For this study, we use the simple choice $\Phi = 1$, implying that convection is always active (and producing a deep moisture flux) whenever $q_1 > q_2$. The form of the parameterisation for the convective flux is comparable to that in Muller *et al.* (2009), where a two-layer model is used to examine the relationship between precipitation and total column moisture. Muller *et al.* parameterise precipitation, P, in terms of the sum of the moisture content over lower and upper layers in the troposphere, with a trigger based on a critical threshold of moisture (q_c) in the lower layer: $P = (q_2 + q_1)\,H\,(q_1 - q_c)$. H is the Heaviside function. This form of parameterisation, linked to total column moisture, can be taken as a basis for the form of the convective flux presented here, where the total column moisture is used as a proxy for precipitation. A more realistic parameterisation of the flux would be modelled on a tanh-style function where convection switches on once a critical threshold of moisture is exceeded, and thereafter the total column moisture would increase monotonically with Φ, consistent with observations of convective rainfall (Neelin *et al.*, 2009).

2.1 | Reduced two-layer model of Indian monsoon onset

For the remainder of this study, we consider a reduced version of this model, spatially one-dimensional but evolving in time, which shows the advance of the onset against a constant northwesterly wind in the upper layer. We evaluate the parameters controlling the onset speed and direction, focusing on the evolution of moisture in the upper layer where there is competition between dry advection and rate of convective flux. Specifically, we simulate the moistening of the upper layer by shallow and medium congestus cumulus clouds, which produce little rainfall. Monsoon onset is declared once the total moisture, $q_1 + q_2$, reaches a particular threshold, say q_*. Evaporation and surface processes are represented as a simple relaxation of the boundary layer state. We set $P = 0$, which is appropriate for the pre-monsoon moistening period when precipitation is low. We also assume that all quantities only vary with x and t, that is, taking a vertical slice. Then, the upper-level wind is retained as $(u_2, 0)$, where u_2 is constant. However, the lower-level wind $(0, v_1)$ has no direct, advective effect, since $\partial/\partial y = 0$. Therefore, to account for the moisture input from the low-level flow over the Arabian Sea and surface evaporation, we relax q_1 towards a prescribed $q_e(x)$ on a timescale T_{moist}. The governing equations (Equations 1a,1b), on substituting Equation 2, become

$$\frac{\partial q_2}{\partial t} + u_2\frac{\partial q_2}{\partial x} = +\frac{1}{T_{\text{conv}}}(q_1 - q_2)\,\Phi, \tag{3a}$$

$$\frac{\partial q_1}{\partial t} + \frac{1}{T_{\text{moist}}}(q_1 - q_e) = -\frac{1}{T_{\text{conv}}}(q_1 - q_2)\,\Phi. \tag{3b}$$

In the absence of advection and moisture replenishment ($u_2 = 0 = 1/T_{\text{moist}}$) and taking the simplest case with $\Phi = 1$, the layers mix according to $e^{-2t/T_{\text{conv}}}$. Likewise, in the absence of convection ($1/T_{\text{conv}} = 0$), the lower layer evolves towards q_e according to $e^{-t/T_{\text{moist}}}$.

A lateral boundary condition (Equation 4) is imposed on the upper layer, accounting for the dry inflow from northwest India and Pakistan over the Thar desert. At the northwestern limit of the domain, the air remains sufficiently dry throughout the monsoon period that the lateral condition is considered appropriate:

$$q_2(x = 0, t) = 0. \tag{4}$$

The resulting behaviour is dependent upon the assumed timescales T_{moist} and T_{conv} for moisture replenishment and mixing due to convection. Suitable values of these timescales can be estimated from knowledge of weather systems. For example, assuming that the lifetime of these processes is determined approximately by the efficiency of mixing due to convection, a single convective cloud might last about an hour, a cluster of convective clouds has a lifetime of several hours, and dry intrusions and storms can persist for several days. The timescale for water vapour to become vertically mixed in the clean-air environment surrounding convection is of the order of days, compared with the convective-scale vertical transport of moisture in clouds taking minutes to an hour (Tompkins and Craig, 1998). Hence, acknowledging

that the real timescale for adjustment of moisture may range from the convective timescale to the timescale of large-scale flow, we use our model to explore a range of values:

$$1/2 \;\leq\; T_{\text{conv}} \;\leq 7 \text{ days}. \tag{5}$$

Similar estimates are needed for setting T_{moist}. In the absence of convection, the assumed lower-layer profile q_e is replenished by evaporation from a saturated surface. For shallow standing water, evaporation is estimated to moisten a boundary layer on a timescale of hours, whereas for moist vegetated layers the timescale would be longer, of the order of several days (Goutorbe *et al.*, 1994). Again, in the absence of convection, changes to the strength or humidity of the inflow from the Arabian Sea might adjust q_e on a timescale of days to a week. We thus take

$$1/2 \;\leq\; T_{\text{moist}} \;\leq 7 \text{ days}. \tag{6}$$

The quantity $q_e(x)$ represents an equilibrium state of the lower layer in the absence of convection. Changing q_e will alter the equilibrium humidity, effectively increasing or decreasing the depth of the lower layer. Here, the simplest choice of $q_e = 1$ is taken. Further work (Recchia, 2020) investigates profiles of the form $1 - e^{-x/L}$ for a length-scale L, to account for the dryness present in northwest India, compared with the higher levels of humidity in southeast India.

For the experiments, the system is initialised in an equilibrium state, which can be determined analytically from Equations 3a,3b with $\partial/\partial t = 0$. We derive the equilibrium solutions in the following Section 2.2.

2.2 | Equilibrium solution

Analytical solutions can be found for long timescales when the system has reached a state of convective equilibrium. A length-scale L_{mon}, defined in terms of the speed u_2 and timescales T_{conv}, T_{moist} (Equation 7), emerges from the solutions. This parameter L_{mon} represents the length-scale of the monsoon system and has typical values in the range 500–5,000 km. A similar length-scale is proposed by Zhou and Xie (2018) to describe the extent of a monsoon over an idealised continent, in terms of a balance between upper-level advection of cool air and a timescale for convective adjustment to quasi-equilibrium. A key difference is that Zhou and Xie (2018) use the thermal budget to derive their model, whereas here we use the water budget:

$$L_{\text{mon}} = u_2 \left(T_{\text{conv}} + T_{\text{moist}}\right). \tag{7}$$

The equilibrium solution for the system of Equations 3a,3b can be found by setting $\partial/\partial t = 0$ and solving for q_1 and q_2, with $\Phi = 1$ and $q_e = 1$. These solutions will make up the initial conditions for several of the experiments conducted. The solutions, in terms of the length-scale L_{mon}, are

$$q_2 = 1 - e^{-x/L_{\text{mon}}}, \tag{8a}$$

$$q_1 = 1 - e^{-x/L_{\text{mon}}} \left(\frac{T_{\text{moist}}}{T_{\text{conv}} + T_{\text{moist}}}\right). \tag{8b}$$

The relative sizes of T_{conv} and T_{moist} only affect the upper layer q_2 as part of the monsoon length-scale L_{mon}. If $T_{\text{conv}} \gg T_{\text{moist}}$, then the solution for the lower layer can be reduced to $q_1 \approx 1 - e^{-x/L_{\text{mon}}} (T_{\text{moist}}/T_{\text{conv}}) \approx 1$. Conversely, if $T_{\text{moist}} \gg T_{\text{conv}}$, then $q_1 \approx 1 - e^{-x/L_{\text{mon}}} = q_2$. When $T_{\text{moist}} = T_{\text{conv}}$, the upper-layer solution remains unchanged, but the lower-layer solution simplifies to $q_1 = 1 - \frac{1}{2} e^{-x/L_{\text{mon}}}$.

At $x = 0$, representing northwest India, the upper-layer solution is zero ($q_2 = 0$), but the lower-layer solution is $q_1 = T_{\text{conv}}/\left(T_{\text{conv}} + T_{\text{moist}}\right)$, which reduces to $q_1 = 1/2$ when $T_{\text{conv}} = T_{\text{moist}}$. If we consider the limiting behaviour when $x \to \infty$, then $e^{-x/L_{\text{mon}}} \to 0$ and thus $q_2 \to 1$, $q_1 \to 1$. Therefore, with an infinitely large domain at a long timescale, both the upper- and lower-layer solutions tend towards the same limiting value.

2.3 | Small-time solution

It is difficult to derive solutions analytically for the system of Equations 3a,3b representing the reduced two-layer model, except for the steady-state case. Thus, the solutions for the time-dependent case will be derived numerically. In order to understand the behaviour of the system after a small amount of time, we rewrite q_1 and q_2 as Taylor series:

$$q_2(x,t) = q_{20}(x) + t q_{21}(x) + \frac{t^2}{2} q_{22}(x) + \ldots, \tag{9a}$$

$$q_1(x,t) = q_{10}(x) + t q_{11}(x) + \frac{t^2}{2} q_{12}(x) + \ldots. \tag{9b}$$

The lateral boundary condition on the upper layer, accounting for dry inflow in northwest India, is taken following Equation 4, so that $q_{20} = 0$ at $x = 0$. We set arbitrary initial conditions on the upper and lower layers, so that the initial-layer moisture contents are defined as functions of x:

$$q_2 = q_{20}(x) \quad \text{at } t = 0, \tag{10a}$$

$$q_1 = q_{10}(x) \quad \text{at } t = 0. \tag{10b}$$

Substituting the series for q_2, q_1 (Equations 9a,9b) into the system of Equations 3a,3b with $\Phi = 1$, applying the boundary and initial conditions (Equations 10a,10b) and equating the powers of t, the series becomes Equations 11a,11b, where the primes represent a derivative with respect to x:

$$q_2 = q_{20} + t\left(\frac{1}{T_{\text{conv}}}(q_{10} - q_{20}) - u_2 q'_{20}\right) + \frac{t^2}{2}\Big(-\frac{2}{T_{\text{conv}}^2}(q_{10} - q_{20}) - \frac{1}{T_{\text{conv}}T_{\text{moist}}}(q_{10} - q_{\text{e}}) - \frac{u_2}{T_{\text{conv}}}\left(q'_{10} - 2q'_{20}\right) + u_2^2 q''_{20}\Big) + \dots, \tag{11a}$$

$$q_1 = q_{10} + t\left(-\frac{1}{T_{\text{conv}}}(q_{10} - q_{20}) - \frac{1}{T_{\text{moist}}}(q_{10} - q_{\text{e}})\right) + \frac{t^2}{2}\left\{\left(\frac{2}{T_{\text{conv}}^2} + \frac{1}{T_{\text{conv}}T_{\text{moist}}}\right)(q_{10} - q_{20}) + \left(\frac{1}{T_{\text{conv}}T_{\text{moist}}} + \frac{1}{T_{\text{moist}}^2}\right)(q_{10} - q_{\text{e}}) - \frac{u_2 q'_{20}}{T_{\text{conv}}}\right\} + \dots. \tag{11b}$$

The small-time deviation from $(q_1, q_2) = (q_{10}, q_{20})$ implies the initial direction of monsoon onset, defined as a threshold of total moisture, which may take the form of a front.[1]

We undertake experiments beginning from an equilibrium state (Equations 8a,8b) in terms of parameters T_{conv}, T_{moist}, and u_2. Then we vary the forcing so the that the system is now described in terms of parameters $\tilde{T}_{\text{conv}}$, $\tilde{T}_{\text{moist}}$, and $\tilde{u}_2$, where the tilde notation represents a change in the respective parameter. A new equilibrium state is reached, as modelled by Equations 8a,8b, but now in terms of $\tilde{T}_{\text{conv}}$, $\tilde{T}_{\text{moist}}$, and $\tilde{u}_2$. The monsoon length-scale changes from L_{mon} to $\tilde{L}_{\text{mon}}$, as the system transitions from an initial to a new equilibrium state.

The development of the system after a small time can be determined using the series in Equations 11a,11b. The initial conditions (q_{20}, q_{10}) are in terms of initial parameters T_{conv}, T_{moist}, and u_2, whilst the small-time Equations 11a,11b are in terms of varied parameters $\tilde{T}_{\text{conv}}$, $\tilde{T}_{\text{moist}}$, and $\tilde{u}_2$. So taking Equations 11a,11b with $T_{\text{conv}} = \tilde{T}_{\text{conv}}$, $T_{\text{moist}} = \tilde{T}_{\text{moist}}$, and $u_2 = \tilde{u}_2$, with initial conditions $q_{20} = 1 - e^{-x/L_{\text{mon}}}$ and $q_{10} = 1 - e^{-x/L_{\text{mon}}} \cdot T_{\text{moist}}/(T_{\text{conv}} + T_{\text{moist}})$, gives

$$q_2 = 1 - e^{-x/L_{\text{mon}}} + t\left(\frac{e^{-x/L_{\text{mon}}}}{T_{\text{conv}} + T_{\text{moist}}}\right)\left(\frac{T_{\text{conv}}}{\tilde{T}_{\text{conv}}} - \frac{\tilde{u}_2}{u_2}\right) + \dots, \tag{12a}$$

$$q_1 = 1 - e^{-x/L_{\text{mon}}}\left(\frac{T_{\text{moist}}}{T_{\text{conv}} + T_{\text{moist}}}\right) + t\left(\frac{e^{-x/L_{\text{mon}}}}{T_{\text{conv}} + T_{\text{moist}}}\right)\left(\frac{T_{\text{moist}}}{\tilde{T}_{\text{moist}}} - \frac{T_{\text{conv}}}{\tilde{T}_{\text{conv}}}\right) + \dots. \tag{12b}$$

We can now describe the state of the system initially, after a small amount of time, and after a long time. We begin with an equilibrium state (Equations 8a,8b) in terms of parameters T_{conv}, T_{moist}, and u_2. Then we vary the forcing so $T_{\text{conv}} \to \tilde{T}_{\text{conv}}$, $T_{\text{moist}} \to \tilde{T}_{\text{moist}}$, and $u_2 \to \tilde{u}_2$. Equations 12a,12b describe the system as it responds to the change in forcing. The final state of the system is described by the equilibrium solutions (Equations 8a,8b), but in terms of parameters $\tilde{T}_{\text{conv}}$, $\tilde{T}_{\text{moist}}$, and $\tilde{u}_2$. From these expressions for different states of the idealised monsoon system, the initial speed with which the monsoon onset propagates over India can be determined. Also, we can find the time taken for the monsoon system to adjust from the initial conditions (representing pre-onset) to the final equilibrium state (representing the full monsoon).

2.4 | Definition of monsoon onset

The definition of monsoon onset used here is based on the adjusted total moisture over both layers, using a threshold of $(q_1 + q_2)/2 = 0.5$. Once the total moisture exceeds this threshold, it is regarded as the monsoon onset.

The total moisture is a more relevant quantity for determining onset than solely the upper-level moisture. Although the threshold value is an arbitrary choice, it is justified because the direction of propagation and shape of the onset contour is key. Using a different threshold value would move the position of the contour spatially, but it would not alter the shape and direction of travel.

2.5 | Initial onset speed

Here, we derive an expression for the initial speed (v) at which the monsoon onset "front" propagates across India in our model. Suppose there is some quantity $Q(x, t)$ with small-time representation $Q_0(x) + tQ_1(x) + \dots$. The

[1]Note that, unless $q_{10}(0) = 0$ and $q'_{20}(0) = 0$, the terms of order t (i.e., q_{11} and q_{21}) imply that $q_2(0, t) \neq 0$, thus violating the lateral boundary condition. Even if $q_{21}(0) = 0$, it is likely that $q_{22}(0) = 0$, implying $q_2(0, t) \neq 0$. This anomaly can be rectified by performing a separate analysis for the combined limit of small x and small t, revealing the existence of a thin boundary layer that matches Equations 11a,11b, to the lateral boundary condition. The boundary-layer analysis remains valid provided that x is not small. The details of this calculation are not given here: see Recchia (2020).

location at which $Q(x,t) = Q_*$ is tracked, where Q_* represents the threshold of total moisture required for monsoon onset. The location is taken as $x = x_*$ when $t = 0$, so $Q_0(x_*) = Q_*$. The subsequent deviation of x from x_* at small time is tracked by writing $x = x_* + vt$. Then

$$\begin{aligned} Q_* &= Q_0(x_* + vt) + tQ_1(x_* + vt) + \mathcal{O}(t^2), \\ &= Q_0(x_*) + vtQ_0'(x_*) + tQ_1(x_*) + \mathcal{O}(t^2). \end{aligned}$$

However, since $Q_* = Q_0(x_*)$, we can equate the largest remaining terms of $\mathcal{O}(t)$ to give Equation 13:

$$v = -Q_1(x_*)/Q_0'(x_*). \tag{13}$$

Now, $Q(x,t)$ could be taken as q_1, q_2, or indeed $q_1 + q_2$. The total moisture $q_1 + q_2$ is the main focus, due to its importance in defining monsoon onset, which is taken as a threshold of the total moisture. We take $Q = q_1 + q_2$, and determine Q_0 and Q_1 from the appropriate terms in the sum of Equations 12a and 12b. Thus, Equation 13 for the onset speed can be rewritten as

$$v = -\frac{u_2\,(T_{\text{conv}} + T_{\text{moist}})}{(T_{\text{conv}} + 2T_{\text{moist}})}\left(\frac{T_{\text{moist}}}{\tilde{T}_{\text{moist}}} - \frac{\tilde{u}_2}{u_2}\right). \tag{14}$$

Note that the onset speed, v, is independent of x_* in our chosen case with $q_e(x) = 1$. However, this is not true when $q_e(x)$ is spatially varying (Recchia, 2020). Furthermore, the initial onset speed, v, is independent of the varied convective timescale, $\tilde{T}_{\text{conv}}$, which cancels in the addition of Equations 12a and 12b.

2.6 | Adjustment time

The time taken for the system to adjust from its initial equilibrium to a new equilibrium, T_{adj}, can be calculated by dividing the total equilibrium distance travelled, x_{adj}, by the small-time derived onset speed, v, which can be calculated with Equation 14. Thus, $x_* + vT$ can be written, with v being the onset speed and T representing time. Letting $T = T_{\text{adj}}$ and $L = x_{\text{adj}}$, cancelling terms and rearranging, gives the required result.

The distance travelled by the onset "front", x_{adj}, is the difference between the initial location of onset, x_*, and the location of onset at the new equilibrium, $\tilde{x}_*$, following a change to one of the parameters. We track the onset contour, where $Q_* = (q_1 + q_2)/2 = 0.5$, following the definition of onset given in Section 2.4. The location x_* can be determined from the equilibrium solutions by summing Equations 8a,8b and rearranging for x_* in terms of T_{conv}, T_{moist} and L_{mon}. The expression for $\tilde{x}_*$ follows in the same way in terms of $\tilde{T}_{\text{conv}}$, $\tilde{T}_{\text{moist}}$, and $\tilde{L}_{\text{mon}}$. Thus, we find

$$x_{\text{adj}} = \tilde{x}_* - x_*, \tag{15}$$

$$= L_{\text{mon}} \ln\left(\frac{T_{\text{conv}} + T_{\text{moist}}}{T_{\text{conv}} + 2T_{\text{moist}}}\right) - \tilde{L}_{\text{mon}} \ln\left(\frac{\tilde{T}_{\text{conv}} + \tilde{T}_{\text{moist}}}{\tilde{T}_{\text{conv}} + 2\tilde{T}_{\text{moist}}}\right). \tag{16}$$

Now, the final expression for the adjustment time in terms of the initial parameters T_{conv}, T_{moist}, u_2 and the varied parameters $\tilde{T}_{\text{conv}}$, $\tilde{T}_{\text{moist}}$, $\tilde{u}_2$ can be written:

$$T_{\text{adj}} = \left|\frac{x_{\text{adj}}}{v}\right|. \tag{17}$$

3 | EXPLORATION OF ANALYTICAL SOLUTIONS

The relationship between layer moisture content and distance, in terms of the equilibrium solutions (Equations 8a,8b), is explored. The two-layer model is associated with a length-scale, L_{mon}, which emerges from the analytical solutions. Section 3.1 investigates the impact of scaling the equilibrium solutions by the monsoon length-scale, L_{mon}. Another aspect to be explored is the sensitivity of the equilibrium solutions to the timescale parameters T_{conv}, T_{moist}. Different regimes for combinations of long and short timescales can be categorised.

3.1 | Scaling of moisture with distance at equilibrium

Figure 4a shows the variation of moisture in the upper (q_2) and lower (q_1) layers at equilibrium against distance, x, for $T_{\text{conv}} = T_{\text{moist}} = 1$ day and $u_2 = 5\,\text{m}\cdot\text{s}^{-1}$ (corresponding to $L_{\text{mon}} = 864$ km). Also shown for reference is the total moisture, $q_1 + q_2$, and the relaxation profile, $q_e = 1$. A large domain is shown, although the primary region of interest is approximately $0 < x < 3{,}000$ km, representing the length of a transect from northwest to southeast India.

Considering Figure 4a, an adjustment over distance is observed, from the value set by the boundary condition (minimum) to the limiting value as $x \to \infty$ (maximum). In the case $q_e = 1$, at $x = 0$, we have $q_2 = 0$ and $q_1 = 0.5$ (from Equations 8a,8b, with $T_{\text{conv}} = T_{\text{moist}}$ and Equation 4). The maximum value is 1 for both layers. Depending on the value of L_{mon}, and thus T_{conv} and T_{moist}, the distance to reach the maximum moisture content varies (figures not shown). As the timescales are lengthened so that L_{mon}

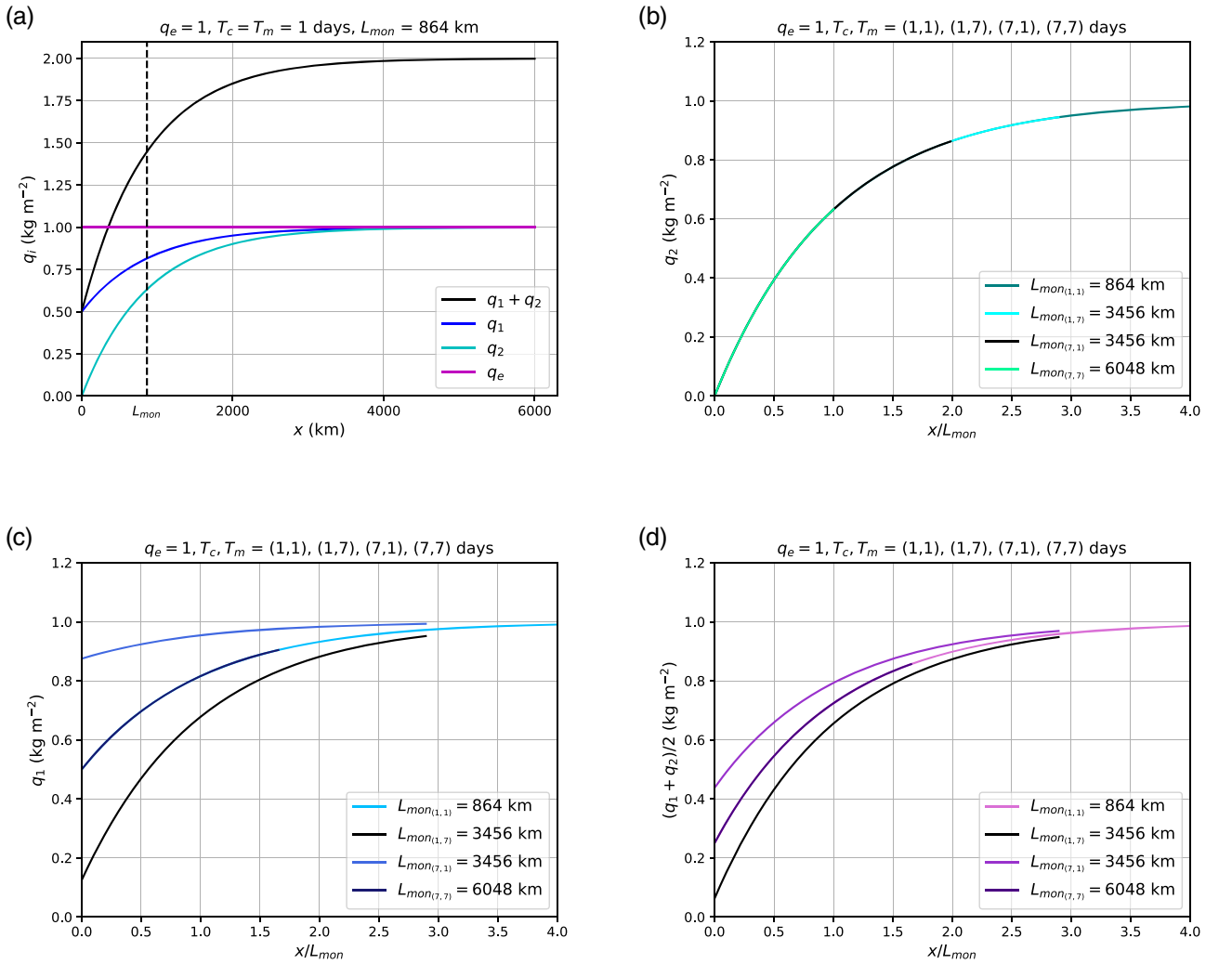

FIGURE 4 Variation of layer moisture q_2, q_1, $q_1 + q_2$ with distance x for (a) T_{conv}=T_{moist} = 1 day and (b,c,d) scaled distance x/L_{mon}, where L_{mon} is the monsoon length-scale: $L_{\text{mon}} = u_2(T_{\text{conv}} + T_{\text{moist}})$. Panel (b) shows the upper-layer moisture (q_2), (c) the lower-layer moisture (q_1), and (d) the total moisture $(q_1 + q_2)/2$, all against (x/L_{mon}) for combinations of T_{conv}, T_{moist}. Produced from equilibrium solutions (Equations 8a,8b), with upper-level wind speed $u_2 = 5\,\text{m}\cdot\text{s}^{-1}$ and moisture replenishment (T_{moist}) and convection (T_{conv}) timescales as labelled

is greater, the distance for the layer moisture contents to reach a constant value increases.

Taking Figure 4a, the x-axis is scaled by the monsoon length-scale, L_{mon}, to investigate whether each of the lines can collapse to its limiting value at the same point. Four monsoon length-scales are considered, relating to four combinations of T_{conv} and T_{moist}, in terms of days: ($T_{\text{conv}} = 1$, $T_{\text{moist}} = 1$), ($T_{\text{conv}} = 1$, $T_{\text{moist}} = 7$), ($T_{\text{conv}} = 7$, $T_{\text{moist}} = 1$), and ($T_{\text{conv}} = 7$, $T_{\text{moist}} = 7$). These pairs of T_{conv}, T_{moist} are denoted in the subplots as $L_{\text{mon}_{(1,1)}}$, $L_{\text{mon}_{(1,7)}}$, $L_{\text{mon}_{(7,1)}}$, and $L_{\text{mon}_{(7,7)}}$, respectively. Figure 4b shows the upper-level moisture, q_2, Figure 4c shows the lower-level moisture, q_1, and Figure 4d shows the total moisture, halved, all against x/L_{mon}.

Solutions for the upper-layer moisture, with $q_e = 1$ (Figure 4b), will always collapse to the same curve when the x-axis is scaled by L_{mon}, regardless of the values taken for timescales T_{conv}, T_{moist}, and thus L_{mon}. This is evident from Equation 8a, which shows that q_2 is a function of x/L_{mon} alone. In Figure 4c, for the lower-layer moisture, it can be seen that the solutions follow the same curve when $T_{\text{conv}} = T_{\text{moist}}$. Again, this is evident from Equation 8b, since $q_1 = 1 - e^{-x/L_{\text{mon}}}/2$ in the case $T_{\text{conv}} = T_{\text{moist}}$. The total moisture follows the lower-layer moisture, with solutions for the total moisture collapsing on to the same curve only when $T_{\text{conv}} = T_{\text{moist}}$, giving the simplified solution $q_1 + q_2 = 2 - 3e^{-x/L_{\text{mon}}}/2$. When $T_{\text{conv}} > T_{\text{moist}}$, the solutions for the lower layer and total moisture lie above the collapsed curve. Conversely, when $T_{\text{conv}} < T_{\text{moist}}$, the solutions for the lower layer and total moisture lie below the collapsed curve. Another point to note is that the lower-layer moisture (q_1) shows a large spread in magnitude with L_{mon}, particularly at small (<0.5) x/L_{mon} values.

3.2 | Sensitivity to timescale parameters at equilibrium

To consider the sensitivity of the system at equilibrium to timescale parameters T_{conv}, T_{moist}, we take the average over the domain $x_0 < x < x_L$ of the layer moisture contents and flux, using Equations 8a,8b. Overbars are used to denote the domain-averaged quantities. We consider a large domain, $0 < x < 100{,}000$ km, to show the limiting behaviour (Figure 5a), and a smaller domain, $0 < x < 3{,}000$ km, representing a transect from north to south India (Figure 5b). The range for both timescales T_{conv} and T_{moist} is 0–3 weeks. Note that the total moisture ($\overline{q_1 + q_2}$) is halved and the flux ($\overline{F}$) is scaled, in order to show results on a similar colour scale to the layer moisture, $\overline{q_1}$, $\overline{q_2}$.

We can see in Figure 5a thatm when a large domain in x is taken, $\overline{q_1} \to 1$, $\overline{q_2} \to 1$, and $(\overline{q_1 + q_2})/2 \to 1$ at small T_{moist}, T_{conv}, in agreement with the limiting behaviour expected. The total moisture, $\overline{q_1 + q_2}$, scaled by 1/2, has contours at approximately 23°, reflecting a greater dependence on T_{moist} compared with T_{conv}. This can be seen by adding Equations 8a and 8b, where a factor of 2 emerges for the parameter T_{moist}. As T_{moist} is decreased, thereby increasing the moisture inflow, the total moisture increases at a greater rate than with decreasing convective timescale, T_{conv}. Generally, the system is more sensitive to the choice of replenishment timescale, T_{moist}, than convective timescale, T_{conv}. In the upper layer, $\overline{q_2}$, decreasing both timescales T_{moist} and T_{conv}, reflecting an increase in moisture inflow and convective activity, leads to more moisture gain in the upper layer. The contours in the $\overline{q_2}$ subplot (Figure 5a) are at 45° from the horizontal, meaning that q_2 has a linear dependence on $T_{\text{conv}} + T_{\text{moist}}$. The contours for the flux ($\overline{F}$) subplot are similar to the upper-layer moisture, $\overline{q_2}$. The flux only depends on the ratio of the upper-level advection, u_2, to the size of the domain, x_L. The flux is greatest when the timescales T_{moist} and T_{conv} are smallest, that is, when the rates of moisture inflow and convection are highest, as would be expected. For the lower layer, $\overline{q_1}$, the moisture content is greatest when $T_{\text{moist}} < 1$ week, irrespective of the value of T_{conv}. As the timescale T_{moist} is increased towards 3 weeks, corresponding to a decreasing rate of moisture inflow, the amount of moisture in q_1 reduces. There is no dependence of q_1 on T_{conv} for large domains ($x_L \gg L_{\text{mon}}$), as seen by the almost horizontal contours in the $\overline{q_1}$ subplot (Figure 5a). This highlights the importance of T_{moist} in determining the lower-layer moisture.

We now consider Figure 5b, which shows the domain averages of the layer moisture contents and flux, over $0 < x < 3{,}000$ km, representing the length of a transect from north to south India. For this choice of domain size, we have $x_L < L_{\text{mon}}$, except at small T_{moist}, T_{conv} (<3.5 days). It is immediately evident from Figure 5b that there are large differences in the total moisture content, $(\overline{q_1 + q_2})/2$, as T_{conv} and T_{moist} vary, compared with Figure 5a. The total moisture increases with decreasing timescale T_{moist}, corresponding to moisture gain in the system when the rate of replenishment to the lower layer is higher, as would be expected. However, in relation to T_{conv}, the total moisture can increase or decrease. We denote a threshold T^*_{moist} (dashed white line), above which the total moisture increases with increasing T_{conv} and below which the total moisture decreases with increasing T_{moist}. When

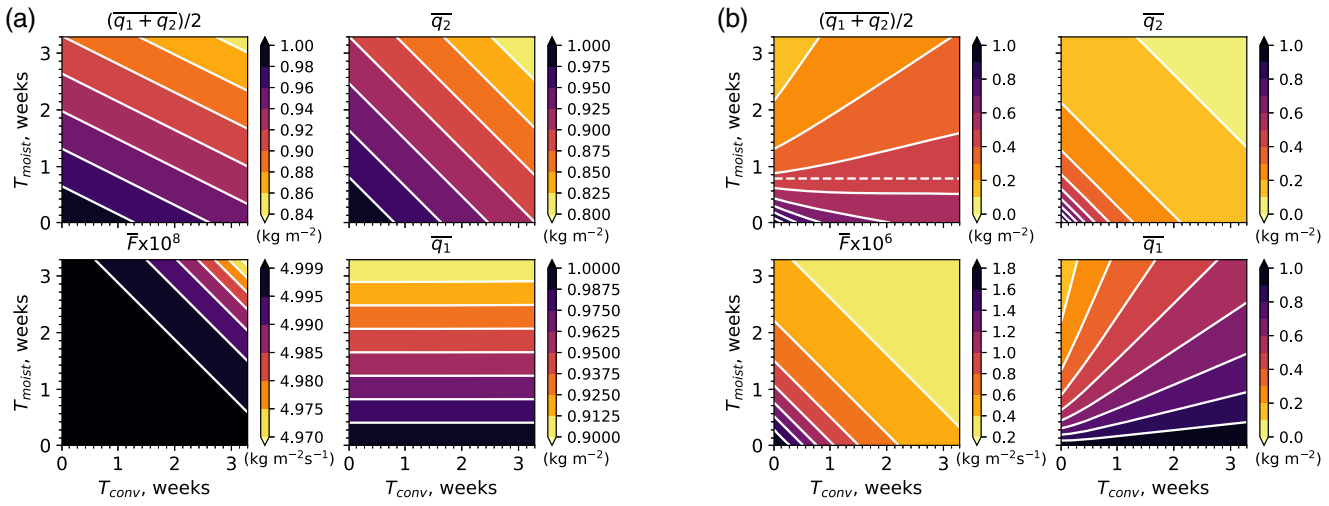

FIGURE 5 Sensitivity of domain-averaged total moisture $\overline{q_1 + q_2}$, flux $\overline{F}$, upper-layer moisture $\overline{q_2}$ and lower-layer moisture $\overline{q_1}$ to varying convective and moisture replenishment timescales, T_{conv} and T_{moist}. $u_2 = 5\,\text{m}\cdot\text{s}^{-1}$, $q_e = 1$ and $\Phi = 1$. Panel (a) is averaged over a large domain $0 < x < 100{,}000$ km, and (b) is averaged over the length of India (north to south) $0 < x < 3{,}000$ km. The dashed white line denotes the threshold T^*_{m}, where the system is in a convective regime below T^*_{m} and an advective regime above T^*_{m}

$(\overline{q_1 + q_2})/2 > T^*_{\text{moist}}$, the system is in an advective regime, with the rate of advection out of the upper layer dominating over the rate of convection from the lower to the upper layer. Otherwise, when $(\overline{q_1 + q_2})/2 < T^*_{\text{moist}}$, the system is in a convective regime, with the rate of convection dominating over the rate of advection. Here, $T^*_{\text{moist}} \approx 5.5$ days.

We suggest that the transition between the two regimes may be a criterion for the establishment of a stable monsoon system. In the pre-onset period, where T_{moist} is high, moist convective events that lead to a drying of the atmosphere cannot be sustained. Once $T_{\text{moist}} < T^*_{\text{moist}}$ (convective regime), convective events act to moisten the atmospheric column and are likely to be maintained. Further details regarding the calculation of T^*_{moist} are given in Section 3.3.

The subplots for $\overline{q_2}$ and $\overline{F}$ in Figure 5b follow the same pattern as for Figure 5a, with both quantities increasing linearly with decreasing T_{moist} and T_{conv}. The contours for the lower layer, $\overline{q_1}$, in Figure 5b are arranged in a radiating pattern. A longer convective timescale, T_{conv}, meaning a slower rate of moisture being transported to the upper layer, allows more moisture to accumulate in the lower layer. In contrast, a longer replenishment timescale, T_{moist}, leads to a reduction in moisture in the lower layer as the rate of moisture inflow is reduced. For very small T_{moist}, T_{conv} (black segment in contour plot), the behaviour for $x_L \gg L_{\text{mon}}$, as in Figure 5a, is recovered.

3.3 | Quantifying advective and convective regimes

T^*_{moist} is interpreted as the threshold between two regimes. Below T^*_{moist}, convection dominates over advection, with higher convective activity leading to moisture gain in the system. Above T^*_{moist}, upper-level advection dominates, with higher convective activity being linked with moisture loss. Shifts in regime in the model represent periods of increased/decreased moisture inflow to the Indian monsoon system. For example, a strengthening of the Somali Jet would increase the moisture inflow from the Arabian Sea (decreasing T_{moist}), thereby shifting below T^*_{moist} and being in a convection-dominant regime.

To derive an expression for the threshold T^*_{moist} (Equation 18), we take the derivative of the domain-averaged total moisture with respect to the convective timescale, $\frac{\partial(\overline{q_1+q_2})}{\partial T_{\text{conv}}}$, at $T_{\text{conv}} = 0$. A nondimensional parameter, ϕ, is introduced to simplify the calculation. We find the value of ϕ using the Newton–Raphson iteration method:

$$T^*_{\text{moist}} = \frac{x_L}{u_2 \phi}, \quad \text{where } \phi \simeq 1.256. \tag{18}$$

From Equation 18, we can see that T^*_{moist} scales with the upper-level advection, u_2, for a given domain size, x_L. This is shown visually in Figure 6. When the upper-level advection is roughly halved (Figure 6a), the threshold T^*_{moist} is approximately doubled, effectively increasing the area that the convection-dominant regime occupies. This is reversed in Figure 6b, with doubling u_2 giving a halved T^*_{moist}. Increasing the upper-level advection gives an increased area of the advection-dominant regime. To summarise, given a domain size of $x_L = 3{,}000$ km and values for the upper-level advection, u_2, we calculate T^*_{moist}:

- with $u_2 = 2\,\text{m}\cdot\text{s}^{-1}$, $T^*_{\text{moist}} \simeq 14$ days,
- with $u_2 = 5\,\text{m}\cdot\text{s}^{-1}$, $T^*_{\text{moist}} \simeq 5.5$ days,
- with $u_2 = 10\,\text{m}\cdot\text{s}^{-1}$, $T^*_{\text{moist}} \simeq 3$ days.

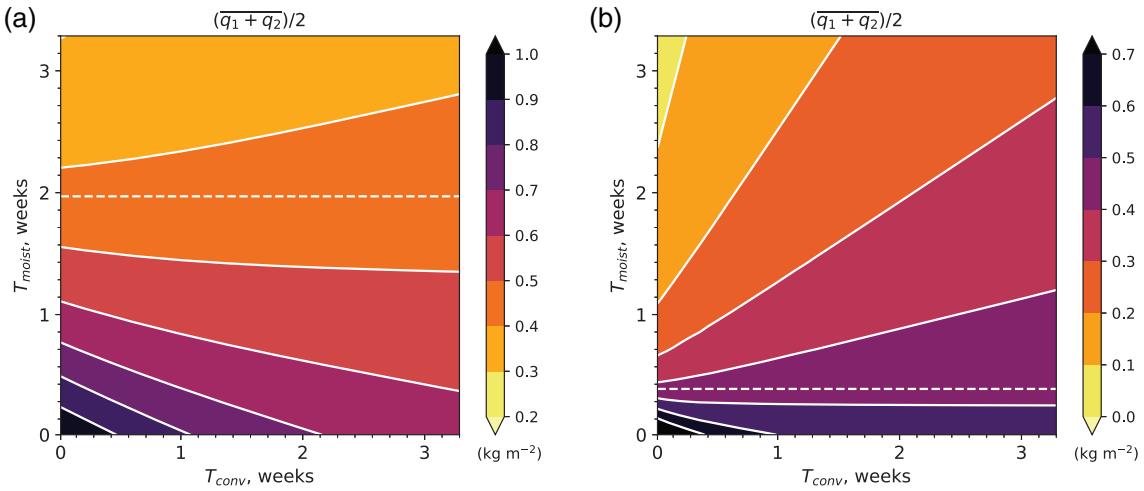

FIGURE 6 Sensitivity of domain-averaged total moisture $\overline{q_1 + q_2}$ to varying convective and moisture replenishment timescales, T_{conv} and T_{moist}: (a) $u_2 = 2\,\text{m}\cdot\text{s}^{-1}$ and (b) $u_2 = 10\,\text{m}\cdot\text{s}^{-1}$. Domain $0 < x < 3{,}000$ km, with $q_e = 1$ and $\Phi = 1$. The dashed white line denotes the threshold T^*_m, where the system is in a convective regime below T^*_m and an advective regime above T^*_m

4 | NUMERICAL SOLUTIONS

The system of Equations 3a,3b is regarded as a model of monsoon onset, where the onset is modelled as a threshold of total moisture, $q_1 + q_2$. We solve Equations 3a,3b numerically with $\Phi = 1$ and $q_e = 1$, varying the rates of moisture inflow (T_{moist}) and advection (u_2) in turn, to isolate the effect of each parameter on the speed and progression of the monsoon onset. The two experiments are initialised in an equilibrium state representing pre-onset conditions using Equations 8a,8b, with parameters T_{moist}, T_{conv}, and u_2, and monsoon length-scale L_{mon}. After initialisation, the system is now described in term of parameters $\tilde{T}_{\text{conv}}$, $\tilde{T}_{\text{moist}}$, and $\tilde{u}_2$, with associated monsoon length-scale $\tilde{L}_{\text{mon}}$. The initial onset speed and time of adjustment from one equilibrium (pre-onset) to a new equilibrium (full monsoon) can be diagnosed numerically (Section 4.1), as well as analytically (Sections 2.5 and 2.6). The numerical results will be compared and contrasted with the analytical theory.

To solve Equations 3a,3b with $\Phi = 1$ and $q_e = 1$ numerically, a fourth-order accuracy Runge–Kutta scheme is used to step the quantities q_2 and q_1 in time. An equispaced finite-difference grid of second-order accuracy is used to approximate the first spatial derivative $\partial/\partial x$. The grid in x has 128 points and the code is run for 5,000 time steps with an interval of 500 s.

The format of the figures showing the results of the experiments is similar to Figure 5, with contoured subplots for lower-layer moisture q_1, flux $F = (1/T_{\text{conv}})(q_1 - q_2)\Phi$ (where $\Phi = 1$), upper-layer moisture q_2, and total moisture $(q_1 + q_2)/2$. Here, the total moisture has been halved and the flux scaled, so that all subplots can use the same levels and colour scale. The x-axis is the distance across India, from northwest ($x = 0$ km) to southeast ($x = 3{,}000$ km) India. The y-axis shows time (weeks). The experiments are run for a sufficiently long time for a new equilibrium to be reached—approximately 4 weeks. The Indian monsoon usually takes 6 weeks to progress over all of India.

The definition of monsoon onset follows Section 2.4, using a threshold of total moisture, $(q_1 + q_2)/2 = 0.5$, which is illustrated as a black contour in the following figures. Once the total moisture reaches this 0.5 threshold (dimensional units of kg·m^{-2}), ideally close to $x = 3{,}000$ km (southeast India), it is regarded as monsoon onset. We expect to see the black contour travelling towards $x = 0$ over time, showing the progression of monsoon onset from southeast to northwest India.

4.1 | Diagnosing onset speed and adjustment time numerically

A moisture-based integral method is used to diagnose the time at which the system reaches a new equilibrium. The integral ($I(t)$ in Equation 19) is constructed to equal 1 at $t = 0$, then decrease over time, tending to zero as $t \to \infty$. The integral is evaluated at each time step. The adjustment time is taken as the time at which the value of the integral drops below a particular threshold, say $q_{\text{threshold}}$. We integrate over $\tilde{x}'_* - x'_*$, where x'_* is related to the initial location of onset and $\tilde{x}'_*$ is related to the final location of onset. The distance $\tilde{x}'_* - x'_*$ is a 100 km wide strip, which encompasses and tracks the onset contour. Taking a wider area is more robust than using a single contour and allows for different monsoon length-scales to be taken into account. $q_{\text{initial}}(x)$ and $q_{\text{final}}(x)$ refer to the total moisture in the initial and final equilibrium states, known analytically, whilst $q(x, t)$ is the time-evolving total moisture, derived numerically.

$$T_{\text{adj}} \equiv t \quad \text{when} \quad I(t) < q_{\text{threshold}}, \quad \text{where}$$
$$I(t) = \frac{1}{\tilde{x}'_* - x'_*} \int_{x'_*}^{\tilde{x}'_*} \left| \frac{q(x,t) - q_{\text{final}}(x)}{q_{\text{initial}}(x) - q_{\text{final}}(x)} \right| dx. \tag{19}$$

Another method based on the location of the onset contour (x_*) was also tested, using the expression $(x_* - x_{*_{\text{final}}})/(x_{*_{\text{initial}}} - x_{*_{\text{final}}})$. However, using the location of a single contour was deemed more sensitive and less robust than the moisture-based integral method.

To diagnose the onset speed, we divide the adjustment distance x_{adj} (Equation 16, derived analytically from the equilibrium solutions) by T_{adj}, which is determined numerically following Equation 19. Note that a negative value of onset speed is expected, indicating a direction towards negative x, reflecting the real-world onset travelling from southeast to northwest India.

5 | EXPERIMENT I: INCREASING THE RATE OF MOISTURE INFLOW

At pre-onset (early May), the low-level southwesterly winds increase in speed and depth, bringing an influx of moisture to southeast India, triggering monsoon onset (June). In our model, the effect of increasing the monsoon flux and the depth of monsoon flow can be tested separately, gauging the response of the monsoon onset. The depth of monsoon flow can be varied through the choice of q_e, which we do not consider here. The monsoon flux is determined by the rate of replenishment, occurring on timescale T_{moist}. Decreasing T_{moist} means a greater amount of moisture inflow (higher monsoon flux) from more moist low-level flow and/or increased surface evaporation. The importance of lower tropospheric humidity, which dominates total column water vapour (Holloway and Neelin, 2009; 2010), in convective onset has been well studied (e.g., Schiro and Neelin, 2019).

TABLE 1 Configuration of parameters for varying T_{moist} experiment

u_2 (m·s^{-1})	T_{conv} (days)	T_{moist} (days)	$\tilde{T}_{\text{moist}}$ (days)
5	7	7	3.5
5	2	2	1
5	1	7	3.5

Here, several different options for decreasing the timescale of replenishment are investigated. All other quantities, such as upper-level advection, u_2, are kept constant once the system has been initialised, with only the timescale of replenishment, T_{moist}, being varied to $\tilde{T}_{\text{moist}}$. The combination of timescale values to be tested, within the range noted in Equation 6, is summarised in Table 1. Firstly, initialising with convective (T_{conv}) and replenishment timescales (T_{moist}) of 7 days, the replenishment timescale is then halved to $\tilde{T}_{\text{moist}} = 3.5$ days. This effectively doubles the moisture inflow to the system, which would be expected to trigger monsoon onset and transition to a full monsoon state. The choice of 7 days is at the higher end of the range given in Equation 6 and corresponds to an advective regime (Section 3.3), as $T_{\text{moist}} > T^*_{\text{moist}}$. In this scenario, we would expect a change from the advective regime to the convective regime.

Next, timescales at the lower end of the range are considered, corresponding to a convective regime. We initialise with $T_{\text{conv}} = T_{\text{moist}} = 2$ days and reduce the replenishment timescale to $\tilde{T}_{\text{moist}} = 1$ day, remaining in a convective regime. Finally, an asymmetric configuration is investigated, with $T_{\text{conv}} = 1$ day and $T_{\text{moist}} = 7$ days initially, then, as before, halving the replenishment timescale to $\tilde{T}_{\text{moist}} = 3.5$ days. If unequal values for the convective and replenishment timescales are to be considered, then it could be argued that the convective timescale should be taken as shorter than the replenishment timescale. It is dependent on the definition and/or measurement of either timescale. For example, in our asymmetric case, the replenishment timescale is taken to reflect changes to the Somali Jet, which brings a large moisture influx over the Arabian Sea. Variations in such a robust air current may occur over timescales of a week or more. In contrast, the convective timescale is chosen to represent shorter-lived events, up to a day, such as formation of convective clouds.

5.1 | Numerical results

Solving the system with parameters as per Table 1, for the case $\Phi = 1, q_e = 1$, gives rise to Figure 7. Most importantly, each panel in Figure 7 shows a monsoon onset (black line) defined on a moisture threshold of $(q_1 + q_2)/2 = 0.5$,

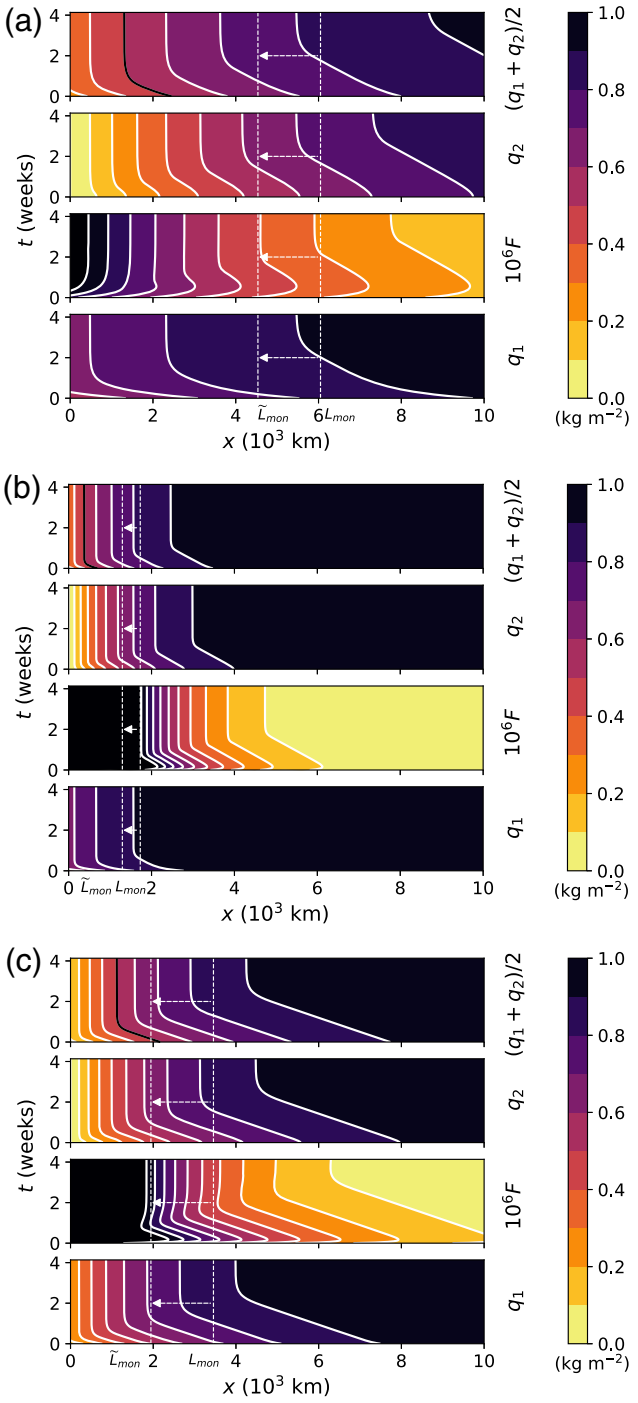

FIGURE 7 Effect of doubling moisture inflow by reducing the relaxation timescale from T_{moist} to $\tilde{T}_{\text{moist}}$, on lower-layer moisture q_1, upper-layer moisture q_2, flux F, and total moisture $q_1 + q_2$, using Equations 3a,3b, with $\Phi = 1$, $q_e = 1$, and $u_2 = 5$ m·s^{-1}, from initial conditions (Equations 8a,8b). (a) T_{conv}=7 days, T_{moist}=7 days, and $\tilde{T}_{\text{moist}}$=3.5 days. (b) T_{conv}=2 days, T_{moist}=2 days, and $\tilde{T}_{\text{moist}}$=1 day. (c) T_{conv}=1 day, T_{moist}=7 days, and $\tilde{T}_{\text{moist}}$=3.5 days. Dashed white lines indicate initial (L_{mon}) and final ($\tilde{L}_{\text{mon}}$) monsoon length-scales. The black contour at $(q_1 + q_2)/2 = 0.5$ indicates the monsoon onset "front"

which travels from southeast to northwest (i.e. in decreasing x direction) India, against a northwesterly wind of $5\,\mathrm{m{\cdot}s^{-1}}$ in the upper layer.

The lower-layer moisture, q_1, behaves similarly for all cases, with increasing moisture content over time until the new equilibrium is reached. This is to be expected, given that the parameter being varied, T_{moist}, represents the moisture flow or monsoon flux into the system, which is being increased. The lower-layer moisture is greatest towards southeast India ($x = 1$), reflecting the real-world monsoon system. The adjustment time and distance are both smaller at low x and larger at high x, increasing proportionally so that the onset speed remains constant. When the initial replenishment timescale, T_{moist}, is shorter (Figure 7b), the lower-layer moisture adjusts faster and over a shorter distance.

The flux, F, increases rapidly at first, responding to the sudden variation of T_{moist}, then decreases over time as a new steady state is reached, and the difference in moisture content between the layers remains constant. This pattern is easier to see in Figure 7a, as the initial increase is very fast in Figures 7b,c. Physically, the sudden increase in moisture could correspond to a short, intense, rainfall event. The flux is greatest towards small x values, where $q_1 - q_2$ is greatest, due to the lateral boundary condition on the upper layer ($q_2 = 0$ at $x = 0$).

The upper-layer moisture evolution, q_2, looks approximately like the lower layer, moistening over time to reach the new equilibrium state and increasing in moisture content with increasing x. Close to $x = 0$, the upper layer is kept dry by the boundary constraint, representing the dry mid–upper level flow from the northwest. For Figure 7a, the upper layer is significantly less moist than the lower layer, due to the longer convective timescale ($T_{\mathrm{conv}} = 7$ days), meaning that less moisture is transported from the lower to the upper layer. Note that there is also advection in the upper layer, acting to remove moisture out of the domain at the southeastern edge.

The total moisture, $(q_1 + q_2)/2$, follows the lower and upper-layer moisture, increasing with t and x. The monsoon length-scales, L_{mon_1} and L_{mon_2}, illustrate the distance the contours travel in order to move from one equilibrium to a new equilibrium. The black contour, delineating monsoon onset, begins in the range $x = 2{,}000$–$3{,}000$ km for Figure 7a,c, which is approximately southeast India. For these parameter choices, the adjustment time between equilibria, representing the time taken for the onset to progress over India, is approximately a week. Although this is considerably faster than the observed monsoon onset, which takes about 6 weeks to progress over India, we interpret the timescale of the monsoon in our model as a response to a change in forcing, rather than representing the entire timescale of monsoon onset. The real-world monsoon onset progresses in a series of stages (Volonté *et al.*, 2020), with bursts of synoptic activity as a response to step changes in forcing. Additionally, the onset in the model travels around 1,000 km, compared with 3,000 km (distance over India). For Figure 7b, the onset contour starts at $x = 1{,}000$–$2{,}000$ km, which is further northwest than the observed monsoon onset. The monsoon length-scales are also shorter and closer together here, when T_{conv} and T_{moist} are of order 1–2 days. The adjustment time (2–3 days) and distance (<500 km) for $T_{\mathrm{conv}} = T_{\mathrm{moist}} = 2$ days is much smaller than for the other cases or the observed monsoon.

Empirically, it seems that the onset speed (ν), that is, the average speed of progression between the initial equilibrium and the new equilibrium, remains approximately independent of x for a given set of parameters. The distance and time of adjustment, x_{adj} and T_{adj}, between the states of equilibrium increase proportionally when contours towards the southeast, at higher x values, are considered.

To quantify monsoon onset, we diagnose the adjustment time, T_{adj}, and onset speed, ν, following Equation 19, with $q_{\mathrm{threshold}} = 0.3$ (i.e. 70%). The system is somewhat sensitive to the choice of $q_{\mathrm{threshold}}$, with different threshold values scaling the numerical results by a constant factor. Figure 8 shows the convergence of Equation 19 with time in weeks. The time needed for the system to adjust to the new equilibrium is the point at which the curves cross the threshold line, $q_{\mathrm{threshold}}$. The cases where T_{conv} and T_{moist} are longer, of order 7 days, take longer to converge and thus give longer adjustment times, irrespective of $\tilde{T}_{\mathrm{moist}}$. The quickest to converge is $T_{\mathrm{conv}} = T_{\mathrm{moist}} = 2$ days.

5.2 | Application of analytical theory

Calculating the speed of onset ν from Equation 14, with $\tilde{T}_{\mathrm{conv}} = T_{\mathrm{conv}}$ and $\tilde{u}_2 = u_2$:

$$\nu = -\frac{u_2\,(T_{\mathrm{conv}} + T_{\mathrm{moist}})}{(T_{\mathrm{conv}} + 2T_{\mathrm{moist}})}\left(\frac{T_{\mathrm{moist}}}{\tilde{T}_{\mathrm{moist}}} - 1\right), \quad \text{for } \tilde{T}_{\mathrm{moist}} \neq T_{\mathrm{moist}}. \tag{20}$$

If $\tilde{T}_{\mathrm{moist}} < T_{\mathrm{moist}}$, as in these experiments, then $\nu < 0$, corresponding to contours moving to the left (i.e., towards northwest India), as expected. The distance travelled by contours from an initial to a new equilibrium, x_{adj}, from Equation 16, is

$$x_{\mathrm{adj}} = -u_2\left(T_{\mathrm{conv}} + \tilde{T}_{\mathrm{moist}}\right)\ln\left(\frac{T_{\mathrm{conv}} + \tilde{T}_{\mathrm{moist}}}{T_{\mathrm{conv}} + 2\tilde{T}_{\mathrm{moist}}}\right)$$

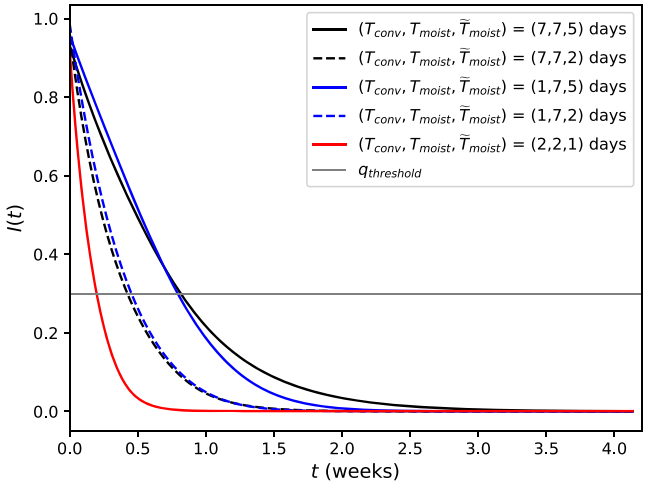

FIGURE 8 Convergence of moisture-based integral $I(t)$ (Equation 19) against time, t, for moisture replenishment timescale varying from T_{moist} to $\tilde{T}_{\text{moist}}$. $\Phi = 1$, $q_e = 1$, and $u_2 = 5\,\text{m}\cdot\text{s}^{-1}$. Adjustment time T_{adj} is the time t at which the value of the integral (y-axis) drops below the threshold, $q_{\text{threshold}}$.

$$+ u_2 (T_{\text{conv}} + T_{\text{moist}}) \ln \left(\frac{T_{\text{conv}} + T_{\text{moist}}}{T_{\text{conv}} + 2T_{\text{moist}}} \right). \quad (21)$$

Similarly, the adjustment time, T_{adj}, from Equation 17, is

$$T_{\text{adj}} = \tilde{T}_{\text{moist}} \left(\frac{T_{\text{conv}} + 2T_{\text{moist}}}{T_{\text{moist}} - \tilde{T}_{\text{moist}}} \right) \left\{ \left(\frac{T_{\text{conv}} + \tilde{T}_{\text{moist}}}{T_{\text{conv}} + T_{\text{moist}}} \right) \times \ln \left(\frac{T_{\text{conv}} + \tilde{T}_{\text{moist}}}{T_{\text{conv}} + 2\tilde{T}_{\text{moist}}} \right) - \ln \left(\frac{T_{\text{conv}} + T_{\text{moist}}}{T_{\text{conv}} + 2T_{\text{moist}}} \right) \right\}. \quad (22)$$

Note that this adjustment time is independent of the upper-level wind speed, u_2. The contour speed (ν) and adjustment length (x_{adj}) are both proportional to u_2, but this dependence cancels out when calculating the adjustment timescale, T_{adj}. For particular cases, Equation 22 can be simplified further. For instance, if an asymmetric case where $T_{\text{conv}} \ll T_{\text{moist}}$ is considered, then

$$T_{\text{adj}} = 2\tilde{T}_{\text{moist}} \ln 2 \simeq 1.4\, \tilde{T}_{\text{moist}}, \quad \text{for} \quad T_{\text{conv}} \ll T_{\text{moist}} \quad \text{and} \quad T_{\text{conv}} \ll \tilde{T}_{\text{moist}}. \quad (23)$$

5.3 | Comparison

Figure 9 shows the results of applying the analytical theory and using numerical techniques to determine the adjustment time, T_{adj} (Figure 9a), and the onset speed, ν (Figure 9b), against $\tilde{T}_{\text{moist}}$. Equations 20 and 22 are used to determine the onset speed, ν, and the adjustment time, T_{adj}, analytically, whilst Equation 19 is used for the numerical results.

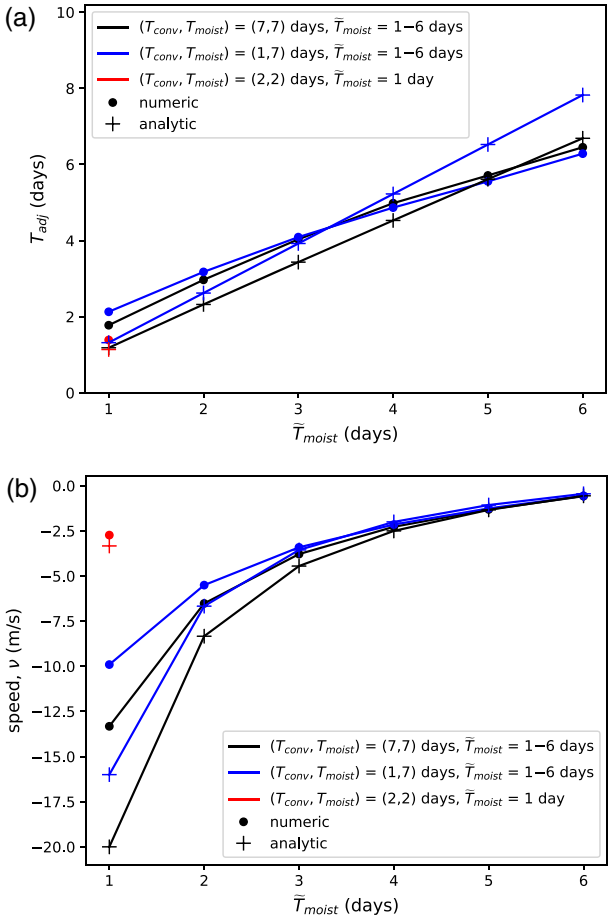

FIGURE 9 Comparing the numerical and analytical derivation of (a) adjustment time, T_{adj}, and (b) onset speed, ν, for varying timescales of moisture replenishment, $\tilde{T}_{\text{moist}}$. $\Phi = 1$, $q_e = 1$, and $u_2 = 5\,\text{m}\cdot\text{s}^{-1}$

Firstly, considering the adjustment time, it can be seen in Figure 9a that T_{adj} is (approximately) linearly related to $\tilde{T}_{\text{moist}}$, such that $T_{\text{adj}} \propto \tilde{T}_{\text{moist}}$. This suggests that a higher rate of moisture inflow, that is, a smaller $\tilde{T}_{\text{moist}}$, corresponds to a faster adjustment time (T_{adj}). In the asymmetric case (with $T_{\text{conv}} = 1$, $T_{\text{moist}} = 7$), this is in agreement with Equation 23. The derived expression estimating T_{adj} from analytical theory (Equation 22) agrees well with the numerical results. This gives confidence in our understanding of the system. The adjustment times for each of the parameter combinations are all below 8 days, compared with the observed monsoon, which takes 6 weeks to transition from first onset to the full monsoon. We suggest interpreting T_{adj} as an adjustment time of the system to changes in the dynamic and thermodynamic forcing. For example, the monsoon system can respond to small differences in the circulation pattern or higher moisture input following a rainfall event (i.e., changing $\tilde{T}_{\text{moist}}$), on a timescale of several days to a week.

Secondly, looking at Figure 9b, the onset speed is close to zero when $\tilde{T}_{\text{moist}} \to T_{\text{moist}}$ and increases when $\tilde{T}_{\text{moist}}$

decreases. Note that the negative value of onset speed is indicating the direction, from southeast to northwest India (i.e. decreasing x direction). The rate of increase in speed becomes greater towards $\tilde{T}_{\text{moist}} = 1$ day. This is particularly evident in the analytical theory. Considering the analytical expression for onset speed, Equation 20, it can be seen that $\nu \to 0$ as $\tilde{T}_{\text{moist}} \to T_{\text{moist}}$, and $\nu \to -\infty$ as $\tilde{T}_{\text{moist}} \to 0$. The numerical results mostly agree with the analytical results, except in terms of onset speeds where $\tilde{T} < 1$ day. In terms of the real-world monsoon, speeds of $<5\,\text{m}\cdot\text{s}^{-1}$ are more rational, indicating that timescales of $T_{\text{moist}} = 7$ days and $\tilde{T}_{\text{moist}} = 3$–4 days are more representative.

We conclude that the analytical expressions for onset speed, ν (Equation 20), and adjustment timescale, T_{adj} (Equation 22), are useful predictors of the actual behaviour.

6 | EXPERIMENT II: VARYING UPPER-LEVEL ADVECTION

Here, the role that the dry intrusion from northwest India plays in moderating the onset of the monsoon is investigated. These dry intrusions can slow the progress of monsoon onset, leading to monsoon breaks and potentially drought (Bhat, 2007; Krishnamurti *et al.*, 2010; Parker *et al.*, 2016). Conversely, a weakening dry intrusion would allow the monsoon onset to propagate to the northwest at a greater speed. Using our model, the effect a dry intrusion has on the monsoon onset can be tested by varying the upper-level advection, u_2, to $\tilde{u}_2$. Table 2 summarises the parameter configurations that will be investigated. Firstly, the system will be initialised with $T_{\text{conv}} = T_{\text{moist}} = 7$ days and $u_2 = 5\,\text{m}\cdot\text{s}^{-1}$, then the strength of the upper-level advection will be increased to $\tilde{u}_2 = 7.5\,\text{m}\cdot\text{s}^{-1}$, indicating a strengthening dry intrusion. The second configuration is similar, but the upper-level advection is halved. Finally, a reduction of the upper-level wind speed is considered, in an asymmetric case, with $T_{\text{conv}} = 1$ day and $T_{\text{moist}} = 7$ days.

6.1 | Numerical results

The system is solved with parameters as per Table 2. Figure 10 shows the results. An onset propagating from

TABLE 2 Configuration of parameters for varying u_2 experiment

T_{conv} (days)	T_{moist} (days)	u_2 ($\text{m}\cdot\text{s}^{-1}$)	$\tilde{u}_2$ ($\text{m}\cdot\text{s}^{-1}$)
7	7	5	7.5
7	7	5	2.5
1	7	5	2.5

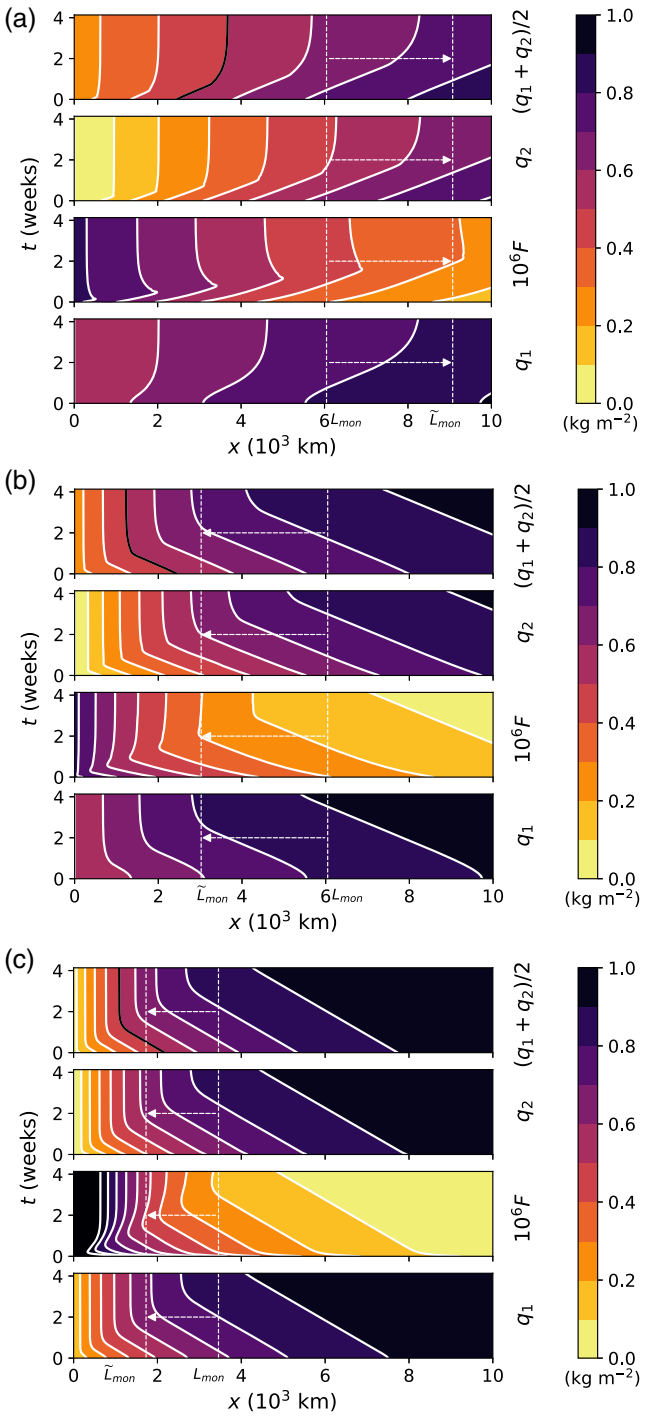

FIGURE 10 Effect of varying upper-level advection from u_2 to $\tilde{u}_2$ on lower-layer moisture q_1, upper-layer moisture q_2, flux F, and total moisture $q_1 + q_2$, using Equations 3a,3b, with $\Phi = 1$ and $q_e = 1$, from initial conditions (Equations 8a,8b). (a) T_{conv}=7 days, T_{moist}=7 days, u_2=5 $\text{m}\cdot\text{s}^{-1}$, and $\tilde{u}_2$=7.5 $\text{m}\cdot\text{s}^{-1}$. (b) T_{conv}=7 days, T_{moist}=7 days, u_2=5 $\text{m}\cdot\text{s}^{-1}$, and $\tilde{u}_2$=2.5 $\text{m}\cdot\text{s}^{-1}$. (c) T_{conv}=1 day, T_{moist}=7 days, u_2=5 $\text{m}\cdot\text{s}^{-1}$, and $\tilde{u}_2$=2.5 $\text{m}\cdot\text{s}^{-1}$. Dashed white lines indicate initial (L_{mon}) and final ($\tilde{L}_{\text{mon}}$) monsoon length-scale. The black contour at $(q_1 + q_2)/2 = 0.5$, indicates the monsoon onset "front"

southeast to northwest is shown by the black contour when the upper-level advection is decreased, for example, in Figures 10b,c.

However, when the upper-level advection is increased, for example, in Figure 10a, a front travelling in the reverse direction (i.e., northwest to southeast) is observed. This highlights the role that dry intrusions can play in halting the progress of the Indian monsoon, potentially leading to monsoon breaks (Bhat, 2007; Krishnamurti *et al.*, 2010).

Considering Figure 10a, it can be seen that the lower and upper moisture, and hence the total moisture, decreases over time until a new equilibrium state is reached. It is particularly evident in q_2. This is not surprising, as the strong upper-level advection acts to remove moisture at the southeastern edge of the domain. In both the upper and lower layer, there is a moisture gradient from northwest to southeast, with moisture content increasing with increasing x. The flux increases at a reasonably fast rate initially. This is in response to the reduction of moisture in the upper layer as advection strengthens. Then, the flux decreases more gradually to its steady-state value. For the total moisture subplot, a reverse onset is observed, with the total moisture decreasing, as upper-level advection is dominant over the timescale of moisture inflow or convection. The monsoon length-scale, L_{mon}, increases.

For the cases with a southeast to northwest propagating onset, Figure 10b,c, the lower, upper, and total moisture contents all increase at a similar rate over time. Weakening of the upper-level winds allows moisture to accumulate in the layers. The adjustment time and distance, based on the black contour, from the initial to the new equilibrium are similar for these cases, taking 1–2 weeks to progress about 1,000 km. Moreover, the adjustment time and distance for Figure 10a seems comparable to that of Figure 10b, albeit in the opposing direction. The system adjusts faster and the onset travels a shorter distance than the observed monsoon. The upper-level moisture, q_2, is zero at the northwest limit, due to the boundary condition. When $T_{\text{conv}} = T_{\text{moist}} = 7$ days, the low-level moisture is fairly high at low x. For Figure 10b,c, the flux for $x >$ 3,000 km decreases over time. At lower x values, the contours for the flux decrease below the new equilibrium value, then increase slightly.

Applying the convergence test (Equation 19), with $q_{\text{threshold}} = 0.1$, the adjustment time and onset speed can be determined. The results of this test are shown in Figure 11. Note that several other combinations of parameters have been included, compared with Table 2. The shortest adjustment times and fastest convergence are seen with $T_{\text{conv}} = T_{\text{moist}} = 2$ days. However, the choice of $\tilde{u}_2$ has a significant impact here, with $\tilde{u}_2 = 10\,\text{m}\cdot\text{s}^{-1}$ converging much faster than $\tilde{u}_2 = 2\,\text{m}\cdot\text{s}^{-1}$.

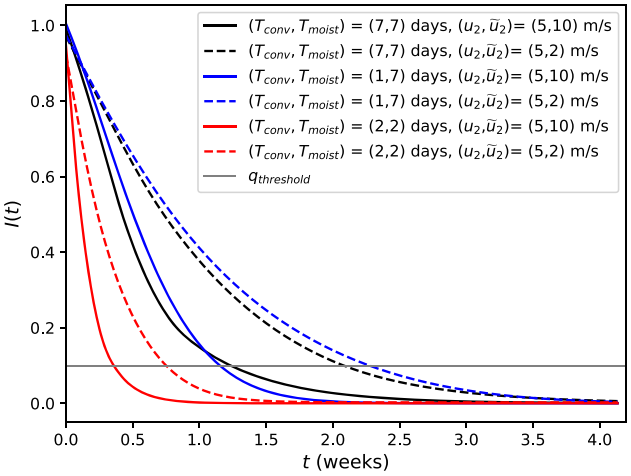

FIGURE 11 Convergence of moisture-based integral $I(t)$ (Equation 19) against time, t, for varying upper-level wind speed from u_2 to $\tilde{u}_2$. $\Phi = 1$ and $q_e = 1$. Adjustment time T_{adj} is the time t at which the value of the integral (y-axis) drops below the threshold, $q_{\text{threshold}}$

6.2 | Application of analytical theory

The speed of onset v, on varying the upper-level wind speed from u_2 to $\tilde{u}_2$, is determined from Equation 14:

$$v = \frac{(T_{\text{conv}} + T_{\text{moist}})}{(T_{\text{conv}} + 2T_{\text{moist}})}(\tilde{u}_2 - u_2), \text{ for } \tilde{u}_2 \neq u_2. \tag{24}$$

The distance travelled by contours from an initial to a new equilibrium, x_{adj}, from Equation 16, is

$$x_{\text{adj}} = (\tilde{u}_2 - u_2)(T_{\text{conv}} + T_{\text{moist}}) \ln\left(\frac{T_{\text{conv}} + 2T_{\text{moist}}}{T_{\text{conv}} + T_{\text{moist}}}\right). \tag{25}$$

Thus, the adjustment time, from Equation 17, is given by

$$T_{\text{adj}} = (T_{\text{conv}} + 2T_{\text{moist}}) \ln\left(\frac{T_{\text{conv}} + 2T_{\text{moist}}}{T_{\text{conv}} + T_{\text{moist}}}\right). \tag{26}$$

Note that this adjustment time, for varying u_2, is in fact independent of u_2 itself. For this experiment, T_{adj} depends only on the combination of the replenishment and convective timescales. Also, if the timescales of convection and replenishment are of a similar magnitude, then

$$T_{\text{adj}} = 3T_{\text{moist}} \ln\left(\frac{3}{2}\right) \simeq 1.2\ T_{\text{moist}}, \text{ for } T_{\text{conv}} \sim T_{\text{moist}}. \tag{27}$$

6.3 | Comparison

The results of determining the adjustment time, T_{adj}, and onset speed, v, numerically, compared with the

analytic derivation, are shown in Figure 12 against varying upper-level wind speed, $\tilde{u}_2$. Numerical quantities are determined using Equation 19. Equations 24 and 26 are used to find the adjustment time and onset speed following the analytical theory.

The analytical theory (Equation 26) gives the adjustment time, T_{adj}, independently of the upper-level advection, u_2, $\tilde{u}_2$, which can be seen in Figure 12a. The numerically derived adjustment time, however, is not independent of the upper-level wind speed, $\tilde{u}_2$. We see that the numerically derived adjustment time increases nonlinearly as the upper-level wind speed is decreased. Thus, for $\tilde{u}_2 \geq 6\,\text{m}\cdot\text{s}^{-1}$, the numerical and analytical adjustment times agree reasonably well, but for $\tilde{u}_2 < 6\,\text{m}\cdot\text{s}^{-1}$, they diverge. In the numerical case, as $\tilde{u}_2 \to 0\,\text{m}\cdot\text{s}^{-1}$, $T_{\text{adj}} \to \infty$, meaning that the system takes increasingly longer to respond as the upper-level advection is reduced. For the analytical results and the numerical results for $\tilde{u}_2 \geq 6\,\text{m}\cdot\text{s}^{-1}$, the adjustment time is approximately $1.2T_{\text{moist}}$, when $T_{\text{conv}} \sim T_{\text{moist}}$ (following Equation 27). Generally, the system responds on a faster timescale to changes in the thermodynamic forcing ($\tilde{T}_{\text{moist}}$) than to changes in the dynamic forcing ($\tilde{u}_2$).

In terms of onset speed, ν, there is an approximately linear relationship between ν and the upper-level wind speed, $\tilde{u}_2$ (Figure 12b). Larger deviations from the initial upper-level wind speed, $u_2 = 5\,\text{m}\cdot\text{s}^{-1}$, correspond to faster onset speeds, as implied by Equation 24. When $\tilde{u}_2 > u_2$, the onset speed is positive, indicating a direction of travel from northwest to southeast (monsoon retreat), and when $\tilde{u}_2 < u_2$, the onset speed is negative, indicating a direction of travel from southeast to northwest (monsoon onset). There is good agreement between numerically and analytically derived onset speeds, except at low $\tilde{u}_2$ ($< 3\,\text{m}\cdot\text{s}^{-1}$). Furthermore, the calculated onset speeds are representative of the onset speed of the real-world monsoon. We highlight the importance of upper-level advection in moderating the progress of the monsoon onset.

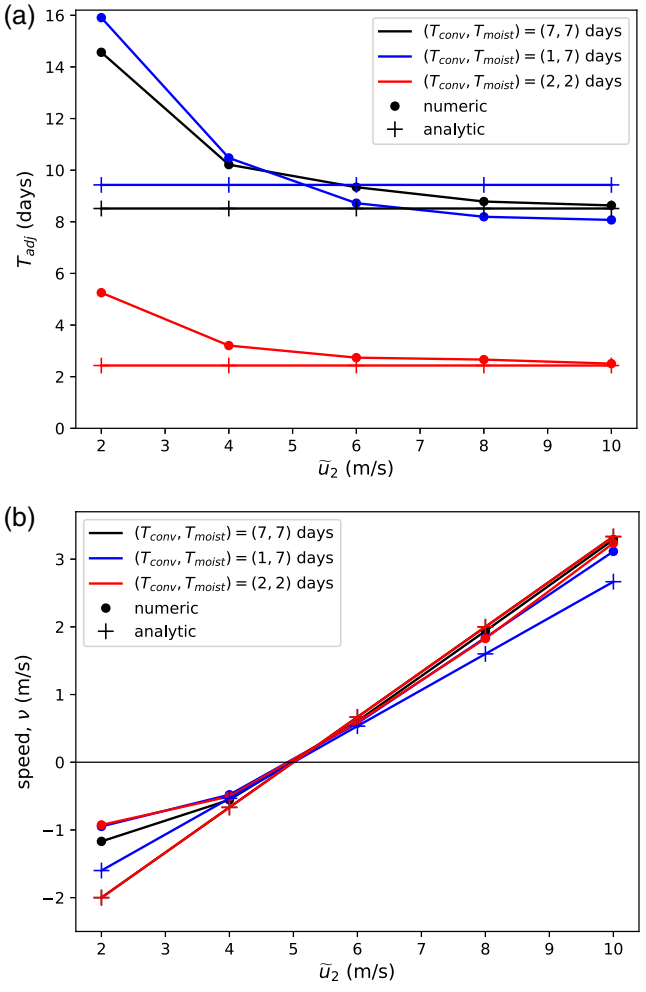

FIGURE 12 Comparing the numerical and analytical derivation of (a) adjustment time, T_{adj}, and (b) onset speed, ν, for varying upper-level wind speed, $\tilde{u}_2$. $\Phi = 1$, $q_e = 1$, and $u_2 = 5\,\text{m}\cdot\text{s}^{-1}$

7 | CONCLUSIONS

A two-layer model of the atmosphere based on moisture conservation was introduced, describing a vertical transect running from northwest to southeast India (x-direction), along which the monsoon onset can propagate. The (reduced) two-layer model consists of a pair of coupled partial differential equations that describe the evolution of the lower- and upper-layer column-integrated moisture contents, $q_1(x,t)$ and $q_2(x,t)$. The simplicity of the model allows the relative roles of convection, low-level moisture replenishment, and upper-layer advection to be evaluated explicitly in the context of monsoon onset. This is a novel approach for studying and quantifying the effect of these key physical processes on the onset and progression of the Indian monsoon.

In the lower layer, the evolution of moisture, $q_1(x,t)$, is determined by the horizontal wind field, including low-level moist inflow from the Arabian Sea, evaporation from the surface, and loss of moisture to the upper layer through a (parameterised) vertical convective flux. The process of low-level inflow is parameterised as a relaxation of the lower layer to a prescribed profile $q_e(x)$, where $q_e(x)$ is interpreted as an equilibrium state in the absence of convection. The relaxation occurs on a timescale T_{moist}. The vertical convective flux is parameterised as a down-gradient flux: $F = (q_1 - q_2)\Phi(q_1, q_2)/T_{\text{conv}}$, where Φ is a nondimensional function representing cloud activity and T_{conv} is the timescale for convection. Values for the timescales T_{moist}, T_{conv} are explored, in the range 1/2–7 days. The upper-layer moisture content, $q_2(x,t)$, is affected by the horizontal wind field, primarily northwesterly dry

advection (u_2), the rate of convection, and the frequency of precipitation. At the northwestern boundary of the transect (where $x = 0$), a completely dry inflow was imposed, so that $q_2(x = 0, t) = 0$.

Analytical solutions can be derived for the steady-state two-layer model. This allows the limiting behaviour of layer moisture (q_1, q_2) to be described on short and long timescales (T_{conv}, T_{moist}), as well as at short and long distances (x). From these equilibrium solutions, a natural monsoon length-scale (L_{mon}) emerges as a combination of the timescales and upper-layer wind speeds, so that $L_{\text{mon}} = u_2 (T_{\text{conv}} + T_{\text{moist}})$. On exploring the variation of layer moisture (q_1, q_2) with distance (x), we find that solutions scale with x/L_{mon}. The upper-layer moisture, q_2, exhibits universal behaviour on scaling with x/L_{mon}, for all choices of timescales T_{conv}, T_{moist}. We also see universal behaviour for the lower layer (q_1) and total moisture ($q_1 + q_2$) when scaled by x/L_{mon}, but only in the case where $T_{\text{conv}} = T_{\text{moist}}$.

We considered the sensitivity of the system at equilibrium to the moisture replenishment and convective timescales, T_{moist} and T_{conv}. We find that the system is more sensitive to the choice of T_{moist}, which represents the low-level physics (advection and evaporation), than the convective physics T_{conv}. The importance of T_{moist} in determining the lower-layer moisture content, q_1, is also highlighted. Two regimes for the steady-state total moisture ($q_1 + q_2$), domain-averaged over India ($\sim 3{,}000$ km), have been identified. When the total moisture is below a threshold T^*_{moist}, it is in a convective regime, with the rate of convection dominating over the rate of advection out of the upper layer. Otherwise, when $q_1 + q_2 > T^*_{\text{moist}}$, it is in an advective regime. The threshold T^*, which can be derived, is inversely proportional to the upper-level wind speed, u_2, for a given domain size. For a domain representing a north–south transect across India (3,000 km) and an upper-level wind speed $u_2 = 5\,\text{m}\cdot\text{s}^{-1}$, we have $T^*_{\text{moist}} \simeq 5.5$ days.

Using the reduced two-layer model, experiments are conducted to investigate the effect of varying parameters on the propagation of the monsoon onset. Experiments are initialised in an equilibrium state with T_{conv}, T_{moist}, u_2, and monsoon length-scale L_{mon}, then we vary the moisture replenishment timescale to $\tilde{T}_{\text{moist}}$ and the upper-level advection to $\tilde{u}_2$ in turn, until the system adjusts to a new equilibrium state, with a new monsoon length-scale $\tilde{L}_{\text{mon}}$. Changing each of these parameters induces monsoon onset, which we define as a threshold of total moisture—a proxy for total column water. For an onset propagating from southeast to northwest India, $L_{\text{mon}} > \tilde{L}_{\text{mon}}$.

Experiments with the reduced two-layer model demonstrate that doubling the rate of low-level moisture flux (by halving T_{moist}) produces a monsoon onset that propagates from southeast to northwest India. Decreasing the upper-layer advection (u_2) allows the monsoon onset to progress at a faster speed to the northwest, whilst increasing the upper-layer advection can result in a monsoon retreat, where the onset front travels in the reverse direction (i.e., to the southeast). This is representative of northwesterly dry intrusions, which are linked with active and break phases during the monsoon as they strengthen or weaken.

Although analytical solutions are not easily derived for the time-evolving system, a combination of alternative methods, including small-time solutions, scaling arguments, and numerical solutions, allows the nature of the onset transition to be understood. These have enabled expressions for the initial speed (v) of the onset contour and an adjustment timescale (T_{adj}) to be derived. We compare expressions derived analytically and numerically, finding that our theoretical understanding agrees well with the numerically derived solutions. The timescale of adjustment (T_{adj}) is the time taken for the system to transition from one equilibrium (pre-onset) to a new equilibrium (full monsoon). The reduced two-layer model takes 1–2 weeks to adjust to a new equilibrium, compared with the observed monsoon onset, which takes approximately 6 weeks to travel from southeast to northwest India. In terms of the real-world monsoon, T_{adj} can be interpreted as the time taken for the monsoon system to adjust to changes in the dynamic and thermodynamic forcing. These changes in forcing occur over time and are linked to bursts of synoptic activity. What we study here is not the whole onset, but the processes of response to changes in forcing. Variations in the large-scale circulation or a higher rate of evaporation following a rainfall event can affect the upper-level advection (u_2) and moisture inflow (T_{moist}) on a timescale of several days to a week. The calculated onset speeds are generally $< 5\,\text{m}\cdot\text{s}^{-1}$, comparable to observed speeds.

It is interesting to note that, for the experiments increasing low-level inflow (T_{moist} to $\tilde{T}_{\text{moist}}$) and varying upper-layer advection (u_2 to $\tilde{u}_2$), the analytically derived adjustment timescale (T_{adj}) depends only on the combination of the replenishment and convective timescales, and not on the initial upper-layer wind speed u_2.

The reduced two-layer model represents an Eulerian view of the evolution of key processes—low-level moist inflow, upper-level advection, and convection—along a vertical cross-section extending from northwest to southeast India. Each of these experiments, varying the processes noted above, reflects changes observed over India around the time of onset, May–June. Changing each of the key parameters causes the system to transition from one equilibrium (pre-onset) to a new equilibrium (full monsoon). Considering the small-time solutions and using scaling arguments, explicit expressions for the onset speed and time of adjustment between equilibria can be derived.

This means the relative importance of each parameter can be assessed. It is found that the adjustment timescale for varying the upper-level advection is in fact independent of the upper-level advection, and that the system is more sensitive to changes in the low-level moisture inflow than the rate of convection. We can also interpret the model in a Lagrangian sense, to explain the shape of the isochrones in Figure 1 around the west coast. Moving from offshore to inland, the moisture replenishment timescale (T_{moist}) increases, with the reduced moisture availability causing the monsoon onset to retreat to the southeast (e.g., June 10 isochrone in Figure 1).

Further work would involve validating the reduced two-layer model against a numerical weather prediction model, such as the Weather Research and Forecasting (WRF) model (as in Recchia, 2020). Questions are raised on how to derive equivalent parameters, such as a convective timescale, from a numerical weather prediction model. The two-layer model could also be adapted to investigate other global monsoons, including the West African monsoon.

ACKNOWLEDGEMENTS

We thank the National Environmental Research Council for funding through its Doctoral Training Partnership (Leeds–York). We acknowledge funding contributions from the INCOMPASS project and the Royal Society. This project is TiPES contribution #99. This project has received funding from the European Union's Horizon 2020 research and innovation programme under grant agreement No. 820970. We also acknowledge ECMWF for providing access to the ERA-Interim reanalysis dataset. We thank the two anonymous reviewers for their constructive comments and suggestions on how to improve the article.

AUTHOR CONTRIBUTIONS

Lucy G. Recchia: data curation; formal analysis; funding acquisition; investigation; methodology; project administration; validation; visualization; writing – original draft; writing – review and editing. **Stephen D. Griffiths:** conceptualization; formal analysis; funding acquisition; methodology; project administration; supervision; writing – review and editing. **Douglas J. Parker:** conceptualization; formal analysis; funding acquisition; methodology; project administration; supervision; writing – review and editing.

ORCID

Lucy G. Recchia https://orcid.org/0000-0002-5907-9468
Douglas J. Parker https://orcid.org/0000-0003-2335-8198

REFERENCES

Bhat, G.S. (2007) The Indian drought of 2002 – a subseasonal phenomenon?. *Quarterly Journal of the Royal Meteorological Society*, 132(621), 2583–2602. https://doi.org/10.1256/qj.05.13.

Birch, C.E., Roberts, M.J., Garcia-Carreras, L., Ackerley, D., Reeder, M.J., Lock, A.P. and Schiemann, R. (2015) Sea-breeze dynamics and convection initiation: the influence of convective parameterization in weather and climate model biases. *Journal of Climate*, 28(20), 8093–8108. https://doi.org/10.1175/JCLI-D-14-00850.1.

Bollasina, M.A. and Ming, Y. (2013a) The general circulation model precipitation bias over the southwestern equatorial Indian Ocean and its implications for simulating the South Asian monsoon. *Climate Dynamics*, 40, 823–838. https://doi.org/10.1007/s00382-012-1347-7.

Bollasina, M.A. and Ming, Y. (2013b) The role of land-surface processes in modulating the Indian monsoon annual cycle. *Climate Dynamics*, 41, 2497–2509. https://doi.org/10.1007/s00382-012-1634-3.

Bollasina, M.A., Ming, Y. and Ramaswamy, V. (2013) Earlier onset of the Indian monsoon in the late twentieth century: the role of anthropogenic aerosols. *Geophysical Research Letters*, 40(14), 3715–3720. https://doi.org/10.1002/grl.50719.

Bombardi, R.J., Pegion, K.V., Kinter, J.L., Cash, B.A. and Adams, J.M. (2017) Sub-seasonal predictability of the onset and demise of the rainy season over monsoonal regions. *Frontiers in Earth Science*, 5, 14. https://doi.org/10.3389/feart.2017.00014.

Dai, A., Li, H., Sun, Y., Hong, L.-C., Chou, C. and Zhou, T. (2013) The relative roles of upper and lower tropospheric thermal contrasts and tropical influences in driving Asian summer monsoons. *Journal of Geophysical Research: Atmospheres*, 118(13), 7024–7045. https://doi.org/10.1002/jgrd.50565.

Ding, Y. and Sikka, D.R. (2006) Synoptic systems and weather. *The Asian Monsoon*, (pp. 131–201). Berlin, Heidelberg: Springer. https://doi.org/10.1007/3-540-37722-0.

Dirmeyer, P.A., Cash, B.A., Kinter, J.L., Jung, T., Marx, L., Satoh, M., Stan, C., Tomita, H., Towers, P., Wedi, N., Achuthavarier, D., Adams, J.M., Altshuler, E.L., Huang, B., Jin, E.K. and Manganello, J. (2012) Simulating the diurnal cycle of rainfall in global climate models: resolution versus parameterization. *Climate Dynamics*, 39, 399–418. https://doi.org/10.1007/s00382-011-1127-9.

Gadgil, S. and Gadgil, S. (2006) The Indian Monsoon, GDP and Agriculture. *Economic and Political Weekly*, 41(47), 4887–4895. http://www.jstor.org/stable/4418949.

Gadgil, S. and Rupa Kumar, K. (2006) The Asian monsoon - agriculture and economy. *The Asian Monsoon*, (pp. 651–683). Berlin, Heidelberg: Springer. https://doi.org/10.1007/3-540-37722-0.

George, G., Rao, D.N., Sabeerali, C.T., Srivastava, A. and Rao, S.A. (2016) Indian summer monsoon prediction and simulation in CFSv2 coupled model. *Atmospheric Science Letters*, 17(1), 57–64. https://doi.org/10.1002/asl.599.

Goswami, B.B. and Goswami, B.N. (2017) A road map for improving dry-bias in simulating the South Asian monsoon precipitation by climate models. *Climate Dynamics*, 49, 2025–2034. https://doi.org/10.1007/s00382-016-3439-2.

Goutorbe, J.P., Lebel, T., Tinga, A., Bessemoulin, P., Brouwer, J., Dolman, A.J., Engman, E.T., Gash, J.H.C., Hoepffner, M., Kabat, P., Kerr, Y.H., Monteny, B., Prince, S., Said, F., Sellers, P.

and Wallace, J.S. (1994) HAPEX–Sahel: a large-scale study of land–atmosphere interactions in the semi-arid tropics. *Annales Geophysicae*, 12(1), 53–64. https://doi.org/10.1007/s00585-994-0053-0.

Gusain, A., Ghosh, S. and Karmakar, S. (2020) Added value of CMIP6 over CMIP5 models in simulating Indian summer monsoon rainfall. *Atmospheric Research*, 232, 104680. https://doi.org/10.1016/j.atmosres.2019.104680.

Holloway, C.E. and Neelin, J.D. (2009) Moisture vertical structure, column water vapor, and tropical deep convection. *Journal of the Atmospheric Sciences*, 66(6), 1665–1683. https://doi.org/10.1175/2008JAS2806.1.

Holloway, C.E. and Neelin, J.D. (2010) Temporal relations of column water vapor and tropical precipitation. *Journal of the Atmospheric Sciences*, 67(4), 1091–1105. https://doi.org/10.1175/2009JAS3284.1.

Holloway, C.E., Woolnough, S.J. and Lister, G.M.S. (2012) Precipitation distributions for explicit versus parametrized convection in a large-domain high-resolution tropical case study. *Quarterly Journal of the Royal Meteorological Society*, 138(668), 1692–1708. https://doi.org/10.1002/qj.1903.

Hoskins, B. and Wang, B. (2006) Large-scale atmospheric dynamics. *The Asian Monsoon*, (pp. 357–415). Berlin, Heidelberg: Springer. https://doi.org/10.1007/3-540-37722-0.

India Meteorological Department & Ministry of Earth Sciences, Government of India, New Delhi, India. (2016) https://mausam.imd.gov.in/ [Accessed 7th November 2016].

Johnson, S.J., Turner, A., Woolnough, S., Martin, G. and MacLachlan, C. (2017) An assessment of Indian monsoon seasonal forecasts and mechanisms underlying monsoon interannual variability in the Met Office GloSea5-GC2 system. *Climate Dynamics*, 48, 1447–1465. https://doi.org/10.1007/s00382-016-3151-2.

Joseph, P.V., Sooraj, K.P. and Rajan, C.K. (2006) The summer monsoon onset process over South Asia and an objective method for the date of monsoon onset over Kerala. *International Journal of Climatology*, 26(13), 1871–1893. https://doi.org/10.1002/joc.1340.

Karmacharya, J., Levine, R.C., Jones, R., Moufouma-Okia, W. and New, M. (2015) Sensitivity of systematic biases in South Asian summer monsoon simulations to regional climate model domain size and implications for downscaled regional process studies. *Climate Dynamics*, 45, 213–231. https://doi.org/10.1007/s00382-015-2565-6.

Krishnamurti, T.N., Thomas, A., Simon, A. and Kumar, V. (2010) Desert air incursions, an overlooked aspect, for the dry spells of the Indian summer monsoon. *Journal of the Atmospheric Sciences*, 67(10), 3423–3441. https://doi.org/10.1175/2010JAS3440.1.

Kumar, K.K., Rupa Kumar, K., Ashrit, R.G., Deshpande, N.R. and Hansen, J.W. (2004) Climate impacts on Indian agriculture. *International Journal of Climatology*, 24(11), 1375–1393. https://doi.org/10.1002/joc.1081.

Lau, K.M., Kim, M.K. and Kim, K.M. (2006) Asian summer monsoon anomalies induced by aerosol direct forcing: the role of the Tibetan Plateau. *Climate Dynamics*, 26, 855–864. https://doi.org/10.1007/s00382-006-0114-z.

Lucas-Picher, P., Christensen, J.H., Saeed, F., Kumar, P., Asharaf, S., Ahrens, B., Wiltshire, A.J., Jacob, D. and Hagemann, S. (2011) Can regional climate models represent the Indian monsoon? *Journal of Hydrometeorology*, 12(5), 849–868. https://doi.org/10.1175/2011JHM1327.1.

Mahmood, R. and Li, S. (2013) Delay in the onset of South Asian summer monsoon induced by local black carbon in an AGCM. *Theoretical and Applied Climatology*, 111, 529–536. https://doi.org/10.1007/s00704-012-0681-3.

Martin, G.M., Klingaman, N.P. and Moise, A.F. (2017) Connecting spatial and temporal scales of tropical precipitation in observations and the MetUM-GA6. *Geoscientific Model Development*, 10(1), 105–126. https://doi.org/10.5194/gmd-10-105-2017.

McGregor, G.R. and Nieuwolt, S. (1998) *Tropical Climatology: An Introduction to the Climates of the Low Latitudes* (2nd edition). Chichester: John Wiley & Sons Ltd.

Meehl, G.A., Arblaster, J.M. and Collins, W.D. (2008) Effects of black carbon aerosols on the Indian monsoon. *Journal of Climate*, 21(12), 2869–2882. https://doi.org/10.1175/2007JCLI1777.1.

Mishra, V., Kumar, D., Ganguly, A.R., Sanjay, J., Mujumdar, M., Krishnan, R. and Shah, R.D. (2014) Reliability of regional and global climate models to simulate precipitation extremes over India. *Journal of Geophysical Research: Atmospheres*, 119(15), 9301–9323. https://doi.org/10.1002/2014JD021636.

Muller, C.J., Back, L.E., O'Gorman, P.A. and Emanuel, K.A. (2009) A model for the relationship between tropical precipitation and column water vapor. *Geophysical Research Letters*, 36(16), L16804. https://doi.org/10.1029/2009GL039667.

Neelin, J.D., Peters, O. and Hales, K. (2009) The transition to strong convection. *Journal of the Atmospheric Sciences*, 66(8), 2367–2384. https://doi.org/10.1175/2009JAS2962.1.

Parker, D.J., Willetts, P., Birch, C., Turner, A.G., Marsham, J.H., Taylor, C.M., Kolusu, S. and Martin, G.M. (2016) The interaction of moist convection and mid-level dry air in the advance of the onset of the Indian monsoon. *Quarterly Journal of the Royal Meteorological Society*, 142(699), 2256–2272. https://doi.org/10.1002/qj.2815.

Recchia, L.G. (2020). Dynamics of the Indian Monsoon onset. PhD thesis, University of Leeds. http://etheses.whiterose.ac.uk/27659/.

Saini, R., Barlow, M. and Hoell, A. (2011) Dynamics and thermodynamics of the regional response to the Indian monsoon onset. *Journal of Climate*, 24(22), 5879–5886. https://doi.org/10.1175/2011JCLI3928.1.

Sanap, S.D. and Pandithurai, G. (2015) The effect of absorbing aerosols on Indian monsoon circulation and rainfall: a review. *Atmospheric Research*, 164–165, 318–327. https://doi.org/10.1016/j.atmosres.2015.06.002.

Schiro, K.A. and Neelin, J.D. (2019) Deep convective organization, moisture vertical structure, and convective transition using deep-inflow mixing. *Journal of the Atmospheric Sciences*, 76(4), 965–987. https://doi.org/10.1175/JAS-D-18-0122.1.

Sperber, K.R., Annamalai, H., Kang, I.-S., Kitoh, A., Moise, A., Turner, A., Wang, B. and Zhou, T. (2013) The Asian summer monsoon: an intercomparison of CMIP5 vs. CMIP3 simulations of the late 20th century. *Climate Dynamics*, 41, 2711–2744. https://doi.org/10.1007/s00382-012-1607-6.

Stephens, G.L., L'Ecuyer, T., Forbes, R., Gettlemen, A., Golaz, J.-C., Bodas-Salcedo, A., Suzuki, K., Gabriel, P. and Haynes, J. (2010) Dreary state of precipitation in global models. *Journal of Geophysical Research: Atmospheres*, 115(D24), D24211. https://doi.org/10.1029/2010JD014532.

Tompkins, A.M. and Craig, G.C. (1998) Time-scales of adjustment to radiative–convective equilibrium in the tropical atmosphere. *Quarterly Journal of the Royal Meteorological Society*, 124(552), 2693–2713. https://doi.org/10.1002/qj.49712455208.

Volonté, A., Turner, A.G. and Menon, A. (2020) Airmass analysis of the processes driving the progression of the Indian summer monsoon. *Quarterly Journal of the Royal Meteorological Society*, 146(731), 2949–2980. https://doi.org/10.1002/qj.3700.

Wang, B. (Ed.) (2006) *The Asian Monsoon*. Heidelberg: Springer. https://doi.org/10.1007/3-540-37722-0.

Willetts, P.D., Marsham, J.H., Birch, C.E., Parker, D.J., Webster, S. and Petch, J. (2017) Moist convection and its upscale effects in simulations of the Indian monsoon with explicit and parametrized convection. *Quarterly Journal of the Royal Meteorological Society*, 143(703), 1073–1085. https://doi.org/10.1002/qj.2991.

Yanai, M., Esbensen, S. and Chu, J.-H. (1973) Determination of bulk properties of tropical cloud clusters from large-scale heat and moisture budgets. *Journal of the Atmospheric Sciences*, 30(4), 611–627. https://doi.org/10.1175/1520-0469(1973)030<0611:DOBPOT>2.0.CO;2.

Zhang, Z., Chan, J.C.L. and Ding, Y. (2004) Characteristics, evolution and mechanisms of the summer monsoon onset over Southeast Asia. *International Journal of Climatology*, 24(12), 1461–1482. https://doi.org/10.1002/joc.1082.

Zhou, W. and Xie, S.-P. (2018) A hierarchy of idealized monsoons in an intermediate GCM. *Journal of Climate*, 31(22), 9021–9036. https://doi.org/10.1175/JCLI-D-18-0084.1.

How to cite this article: Recchia, L.G., Griffiths, S.D. & Parker, D.J. (2021) Controls on propagation of the Indian monsoon onset in an idealised model. *Quarterly Journal of the Royal Meteorological Society*, 1–22. Available from: https://doi.org/10.1002/qj.4165